

The Importance of Being Correlated: Implications of Dependence in Joint Spectral Inference across Multiple Networks

Konstantinos Pantazis¹, Avanti Athreya², William N. Frost³, Evan S. Hill³,
Vince Lyzinski¹

¹ University of Maryland, College Park, Department of Mathematics

² Johns Hopkins University, Department of Applied Mathematics and Statistics

³ Rosalind Franklin University of Medicine and Science, Chicago Medical School, Cell Biology and
Anatomy, and Center for Brain Function and Repair

June 1, 2025

Abstract

Spectral inference on multiple networks is a rapidly-developing subfield of graph statistics. Recent work has demonstrated that joint, or simultaneous, spectral embedding of multiple independent network realizations can deliver more accurate estimation than individual spectral decompositions of those same networks. Little attention has been paid, however, to the network correlation that such joint embedding procedures necessarily induce. In this paper, we present a detailed analysis of induced correlation in a *generalized omnibus* embedding for multiple networks. We show that our embedding procedure is flexible and robust, and, moreover, we prove a central limit theorem for this embedding and explicitly compute the limiting covariance. We examine how this covariance can impact inference in a network time series, and we construct an appropriately calibrated omnibus embedding that can detect changes in real biological networks that previous embedding procedures could not discern. Our analysis confirms that the effect of induced correlation can be both subtle and transformative, with import in theory and practice.

1 Introduction

Networks and graphs, which consist of objects of interest and a vast array of possible relationships between them, arise very naturally in fields as diverse as political science (party affiliations among voters); bioinformatics (gene interactions); physics (dimer systems); and sociology (social network analysis), to name but a few. As such, they are a useful data structure for modeling complex interactions between different experimental entities. Network data, however, is qualitatively distinct from more traditional Euclidean data, and

statistical inference on networks is a comparatively new discipline, one that has seen explosive growth over the last two decades. While there is a significant literature devoted to the rigorous statistical study of single networks, multiple network inference—the analogue of the classical problem of multiple-sample Euclidean inference—is still relatively nascent.

Much recent progress in network inference has relied on extracting Euclidean representations of networks, and popular methods include spectral embeddings of network adjacency [3] or Laplacian [42] matrices, representation learning [19, 41], or Bayesian hierarchical methods [15]. Moreover, many network models [21] allow for important properties of network entities to be hidden, or *latent*, and posit that relationships between entities depend on these latent variables. Such models, known as *latent position networks*, have wide intuitive appeal. For instance, relationships among participants in a social network are a function of the participants’ personal interests, which are typically not directly observed. In these cases, spectral embeddings can provide useful estimates of latent variables, effectively transforming, via eigendecompositions, a non-Euclidean inference problem into a Euclidean one.

For single latent position networks, spectrally-derived estimates of important graph parameters are well-understood, and under mild assumptions, these estimates satisfy classical notions of consistency [44, 42], asymptotic normality [4, 48], and efficiency [48, 47, 53, 5]. More recently, spectral methods have proven useful in multi-sample network inference also, including (non)parametric estimation [15, 49], two-sample hypothesis testing [45, 46, 2, 27], and graph matching [31, 59, 60]. Typically, these methods rely upon separately embedding multiple networks into a lower-dimensional Euclidean space and then aligning the embeddings via Procrustes analysis [18] or point set registration methods [34]. An important issue in multi-sample inference, however, is the leveraging of *multiple* networks both for improved estimation of underlying model parameters and for more streamlined testing across several populations of networks. To this end, a number of recent papers are dedicated to the development of novel techniques for simultaneously embedding several networks into a common Euclidean space, employing spectral graph techniques [26, 35, 52, 1], tensor factorizations [57, 56], multilayer network decompositions [25, 38, 39], and nonparametric Bayesian algorithms [15, 14].

While multisample joint embedding methods allow for accurate graph inference and are often superior to individual separate embeddings [26, 1], there are a number of potential pitfalls in joint embeddings. In particular, network statisticians must confront issues of noisy vertex alignments across graphs [29]; large, high-rank matrices that arise in a joint embedding [13]; the relationship between individual network sparsity and the signal in a joint embedding; and the *induced correlation* across estimates that arise from the joint embedding, the last of which is inevitable in any simultaneous embedding procedure. This induced correlation, and its effect in either masking or amplifying important signal in the context of the omnibus multiple graph embedding procedure (OMNI) [26], is a primary focus of the present paper.

To understand the importance of this induced correlation, it is instructive to recall that theoretical guarantees for most multisample joint embedding procedures hold when the network realizations are independent. Thus, the error bounds for such algorithms often do not apply for correlated networks or network time series. However, when the independent network samples are jointly embedded, correlation across the embedded point clouds is automatically induced (this is the price we pay to circumvent the pairwise Procrustes/registration analysis necessary in separate embedding settings). It is natural, then, to seek a joint em-

bedding technique that induces in independent graphs the same correlation that would be present if edge-wise correlated networks are embedded separately and then aligned. For one, this would allow for the jointly-embedded independent networks to be a more appropriate proxy in embedding space for sequences of non-independent graphs. This, in turn, enables the application of a collection of independent-network inference techniques to the case of correlated networks and network time series. Moreover, experimental results (see Section 5) indicate that well-constructed joint embeddings can better preserve the latent correlation structure across a time series of networks, especially when compared to current methods that do not account for the inherent, pre-existing correlation in the network time series.

To understand this phenomena more rigorously, we consider a specific class of latent position random graphs, the *random dot product graph* [54]. Random dot product graphs have proven to be a theoretically tractable family of latent position networks [3] suitable for modeling a host of complex real-data networks [48, 40, 37]. We consider the omnibus embedding methodology (OMNI) of [26], in which adjacency matrices of multiple independent, vertex-aligned random dot product graphs are inserted as diagonal blocks in a larger matrix M , and a pairwise combination of these adjacency matrices is placed on each off-diagonal block of M . If the common vertex set is of size n , and we have m distinct adjacency matrices, then M is of size $mn \times mn$. Under mild assumptions, M is a random matrix whose conditional expectation is low rank, say rank d , where d does not grow with n , and the omnibus embedding is defined as the d -dimensional eigendecomposition of M given by the scaled eigenvectors of the d largest-magnitude eigenvalues of M . As such, the omnibus embedding is an $mn \times d$ -dimensional matrix, one that provides m distinct representations for the latent attributes of each of the n vertices in the collection of graphs. Because the omnibus embedding is a joint embedding of a matrix with diagonal blocks that consist of pairwise convex combinations of adjacency matrices, the m distinct $n \times d$ blocks in the embedding (there are m such blocks) are correlated.

The major contributions of this paper are as follows. By comparing the omnibus embedding of independent graphs to the separate embeddings of correlated (and subsequently Procrustes-aligned) graphs, we are able to explicitly capture the level of correlation the joint OMNI embedding induces in the limit across independent networks. This, in turn, motivates modifications of the omnibus matrix M that produce more complex correlation structure in the embedded space, enabling higher-fidelity application of the omnibus methodology in real data. This ability to replicate more complicated correlation structure renders the omnibus embedding suitable for inference on network time series, because it permits us to reproduce, via realizations of independent networks, the correlation that is an important component of a time series. The core result underlying each of the above contributions is a novel central limit theorem (Theorem 3) for the row-wise residuals of the estimated latent positions in RDPGs in a very general omnibus embedding framework.

A part of this limit theorem is an explicit formulation of the induced correlation. As an illustration of the power of this correlation in a more general omnibus embedding, we present in Section 5 an analysis of a motor program time series of networks in the the brain of the marine mollusk *Aplysia californica*. The classical omnibus embedding on this time series homogenizes the latent correlation, effectively obscuring important network changes corresponding directly to transitions in animal behavior (from stimulus to gallop and crawl). Our generalized omnibus embedding, however, is flexible enough to permit different weight-

ings of networks over time, and this more general joint inference procedure captures exactly the signal the earlier omnibus embedding misses. Figure 6 and Figure 8 demonstrate this contrast in inferential accuracy between the two.

It is a genuine challenge to design a flexible, easily interpretable inference procedure for analyzing time-varying (or correlated) networks. Moreover, deducing the dependence induced across networks by any given joint network inference methodology is an under-explored area of research in the multiple network literature, and as we demonstrate in Section 5, this dependence can often hide statistically important signal in the data. Our generalized omnibus embedding is a tractable, scalable, transparent inference procedure that correctly identifies important and subtle network changes that its predecessors miss.

Notation: Here, we introduce the notation being used throughout this text. For a positive integer n , we let $[n] = \{1, 2, \dots, n\}$, and let $J_n \in \mathbb{R}^{n \times n}$ be the matrix with all entries identically equal to one. The set of $n \times n$ real orthogonal matrices is denoted by \mathcal{O}_n . We represent a simple (no self-loops or multiple edges), un-weighted and un-directed graph as the ordered pair $g = (V, E)$, where $V = [n]$ represents the set of nodes and $E \subset \binom{[n]}{2}$ the set of edges of the graph; we denote the set of all n -vertex labeled graphs via \mathcal{G}_n . For the graph $g = (V, E)$, we will denote its adjacency matrix via $A \in \{0, 1\}^{n \times n}$; i.e., A_{ij} is equal to 1 if there exists an edge between nodes i and j in g , and 0 otherwise. Where there is no danger of confusion, we will often refer to a graph g and its adjacency matrix A interchangeably. The Kronecker product is denoted by \otimes and the direct sum by \oplus . Finally, the symbols $\|\cdot\|_F$, $\|\cdot\|$, and $\|\cdot\|_{2 \rightarrow \infty}$ correspond to the Frobenius, spectral and two-to-infinity norms respectively.

2 Background

In this section, we will introduce the modeling and spectral embedding frameworks that we build our theory and methods upon.

2.1 Random Dot Product Graphs

The theoretical developments to follow are situated in the context of the *random dot product graph* (abbreviated RDPG) model of [54]. Random dot product graphs are a special case of the more general *latent position random graphs* (LPGs) [22]. Every vertex in a latent position random graph has associated to it a (typically unobserved) *latent position*, itself an object belonging to some (often Euclidean) space \mathcal{X} . Probabilities of an edge between two vertices i and j , p_{ij} , are then a function $\kappa(\cdot, \cdot) : \mathcal{X} \times \mathcal{X} \rightarrow [0, 1]$ (known as the *link function*) of their associated latent positions (x_i, x_j) . Thus $p_{ij} = \kappa(x_i, x_j)$, and edges between vertices arise independently of one another. Given these probabilities, the entries A_{ij} of the adjacency matrix A are conditionally independent Bernoulli random variables with success probabilities p_{ij} . We consolidate these probabilities into a matrix $P = (p_{ij})$, and we write $A \sim P$ to denote this relationship.

In a d -dimensional random dot product graph, the latent space is an appropriately-constrained subspace of \mathbb{R}^d , and the link function is simply the dot product of the two latent d -dimensional vectors. Random dot product graphs are often divided into two types: those

in which the latent positions are fixed, and those in which the latent positions are themselves random. Specifically, we consider the case in which the latent position $X_i \in \mathbb{R}^d$ for vertex i is drawn from some distribution F on \mathbb{R}^d , and we further assume that the latent positions for each vertex are drawn independently and identically from this distribution F . Random dot product graphs have proven to be a tractable and useful model for low-rank latent position networks, and variants of the RDPG model have recently emerged that extend the framework to allow for modeling more complex network topologies [43, 48].

Definition 2.1 (d -dimensional RDPG). *Let F be a distribution on a set $\mathcal{X} \in \mathbb{R}^d$ satisfying $\langle x, x' \rangle \in [0, 1]$ for all $x, x' \in \mathcal{X}$. Let $X_1, X_2, \dots, X_n \sim F$ be i.i.d. random variables distributed via F , and let $P = \mathbf{X}\mathbf{X}^T$, where $\mathbf{X} = [X_1^T | X_2^T | \dots | X_n^T]^T \in \mathbb{R}^{n \times d}$. Let A be a symmetric, hollow adjacency matrix with above diagonal entries distributed via*

$$P(A|\mathbf{X}) = \prod_{i < j} (X_i^T X_j)^{A_{i,j}} (1 - X_i^T X_j)^{1-A_{i,j}}; \quad (1)$$

i.e., conditioned on \mathbf{X} the above diagonal entries are independent Bernoulli random variables with success probabilities provided by the corresponding above diagonal entries in P . The pair (A, \mathbf{X}) is then said to be an instantiation of a d -dimensional Random Dot Product Graph with distribution F , denoted $(A, \mathbf{X}) \sim \text{RDPG}(F, n)$.

To model the setting of multiple correlated RDPGs, we consider pairwise edge-correlated RDPGs as in [37].

Definition 2.2 (ρ -correlated RDPG). *Let F be a distribution on a set $\mathcal{X} \in \mathbb{R}^d$ satisfying $\langle x, x' \rangle \in [0, 1]$ for all $x, x' \in \mathcal{X}$. Let $X_1, X_2, \dots, X_n \sim F$ be i.i.d. random variables distributed via F , and let $P = \mathbf{X}\mathbf{X}^T$, where $\mathbf{X} = [X_1^T | X_2^T | \dots | X_n^T]^T \in \mathbb{R}^{n \times d}$. We say that $(A^{(1)}, \mathbf{X})$ and $(A^{(2)}, \mathbf{X})$ are an instantiation of a ρ -correlated RDPG(F, n) model (written $(A^{(1)}, A^{(2)}, \mathbf{X}) \sim \text{RDPG}(F, n, \rho)$) if*

i. Marginally, $(A^{(1)}, \mathbf{X}) \sim \text{RDPG}(F, n)$ and $(A^{(2)}, \mathbf{X}) \sim \text{RDPG}(F, n)$;

ii. Conditioned on \mathbf{X} , the collection

$$\{A^{(k)}(i, j)\}_{k=1,2, i < j}$$

is mutually independent except that for each $\{i, j\} \in \binom{V}{2}$, $\text{corr}(A_{i,j}^{(1)}, A_{i,j}^{(2)}) = \rho$.

As the correlation is introduced across a pair of networks, it is immediate that we can sample from $(A^{(1)}, A^{(2)}, \mathbf{X}) \sim \text{RDPG}(F, n, \rho)$ by first sampling from $(A^{(1)}, \mathbf{X}) \sim \text{RDPG}(F, n)$, and then conditional on $A^{(1)}$ and \mathbf{X} , independently sampling the edges of $A^{(2)}$ according to the following rubric:

$$\mathbb{P}(A_{i,j}^{(2)} = 1 \mid A_{i,j}^{(1)} = 1, \mathbf{X}) = X_i^T X_j + \rho(1 - X_i^T X_j); \quad (2)$$

$$\mathbb{P}(A_{i,j}^{(2)} = 1 \mid A_{i,j}^{(1)} = 0, \mathbf{X}) = (1 - \rho)X_i^T X_j. \quad (3)$$

This allows for a natural model for correlated, stationary time series of networks $(A^{(t)})_{t \geq 0}$ to be realized as follows. First sample $(A^{(0)}, \mathbf{X})$ according to an $\text{RDPG}(F, n)$ model; then for each $i \geq 0$, conditioned on $A^{(i)}$, and \mathbf{X} generate $A^{(i+1)}$ according to Eq. (2)-(3). Note that by suitably varying ρ and the probabilities in (2)-(3), we can also model non-stationary time series (i.e., allowing the distributions of $A^{(i)}$ and $A^{(j)}$ to differ; see [30] for detail).

Remark 1. *Note that there is a rotational non-identifiability inherent to the RDPG model. Indeed, if $\mathbf{Y} = \mathbf{X}W$ for $W \in \mathcal{O}_d$, then the distribution over graphs induced by Eq. (1) by X and Y are identical; i.e., $\mathbb{P}(A|\mathbf{X}) = \mathbb{P}(A|\mathbf{Y})$ for all A . As inference in the RDPG setting often proceeds by first estimating the latent positions \mathbf{X} , which can only be done up to a rotation factor, this model is not generally suitable for inference tasks that are not rotationally invariant.*

2.2 Spectral graph embeddings

One of the key inference tasks in latent position random graphs (LPGs) is to estimate the unobserved latent positions for each of the vertices based on a single observation of the adjacency matrix of a sufficiently large graph. Since the matrix of connection probabilities for an RDPG is expressible as an outer product of the matrix of true latent positions, and since the adjacency matrix A can be regarded as a “small” perturbation of P , the inference of properties of P from an observation of A is a problem well-suited to spectral methods, such as singular value decompositions, of adjacency or Laplacian matrices. Indeed, these spectral decompositions have been the basis for a suite of approaches to graph estimation, community detection, and hypothesis testing for random dot product graphs. (For a comprehensive summary of these techniques, see [3].) Because of the invariance of the inner product to orthogonal transformations, however, the RDPG exhibits a clear nonidentifiability: latent positions can be estimated only up to an orthogonal transformation. Note that the popular stochastic blockmodel (SBM) can be regarded as a random dot product graph. In an SBM, there are a finite number of possible latent positions for each vertex—one for each block—and the latent position exactly determines the block assignment for that vertex.

Random dot product graphs are often divided into two types: those in which the latent positions are fixed, and those in which the latent positions are themselves random. Specifically, we consider the case in which the latent position $X_i \in \mathbb{R}^d$ for vertex i is drawn from some distribution F on \mathbb{R}^d , and we further assume that the latent positions for each vertex are drawn independently and identically from this distribution F . A common graph inference task is to infer properties of F from an observation of the graph alone. For example, in a stochastic block model, in which the distribution F is discretely supported, we may wish to estimate the point masses in the support of F . In the graph inference setting, however, there are two sources of randomness that culminate in the generation of the actual graph: first, the randomness in the latent positions, and second, *given these latent positions*, the conditional randomness in the existence of edges between vertices.

A rank- d RDPG has a connection probability matrix P that is necessarily low rank (rank d , regardless of the number of vertices in the graph); hence random dot product graphs can be productively analyzed using low-dimensional embeddings. Under mild assumptions, the adjacency matrix A of a random dot product graph approximates the matrix $P = \mathbb{E}(A)$ (to be more precise, $P = \mathbb{E}(A|X)$) in the sense that the spectral norm of $A - P$ can be controlled; see [36, 28]. It is reasonable to ask how close the spectrum and associated invariant subspaces of A are to those of P . Weyl’s Theorem [24] describes how the eigenvalues of A differ from those of P . Sharp bounds on differences between the associated invariant subspaces are fewer, with the Davis-Kahan Theorem [12, 6, 55] perhaps the best known.

Since P is a symmetric, positive definite, rank d -matrix of the form $P = \mathbf{X}\mathbf{X}^T$, the latent

position matrix \mathbf{X} can be written as $\mathbf{X} = U_P S_P^{1/2} W$ for some orthogonal matrix W , where S_P is the diagonal matrix of the d nonzero eigenvalues of P , sorted by magnitude, and U_P the associated eigenvectors. The Davis-Kahan Theorem translates spectral norm bounds on $A - P$ to projection operator bounds between $U_A U_A^T$ and $U_P U_P^T$, and, in turn, into Frobenius norm bounds between U_A and a rotation of U_P [42].

These bounds can be sufficiently sharpened to ensure that the rows of a partial spectral decomposition of A , known as the *adjacency spectral embedding* (ASE) are accurate estimates of the latent positions X_i for each vertex. With this in mind, we define the adjacency spectral embedding (ASE) as follows.

Definition 2.3 (Adjacency Spectral Embedding (ASE)). *Let $d \geq 1$ be a positive integer. The d -dimensional Adjacency Spectral Embedding of a graph $A \in \mathcal{G}_n$ into \mathcal{R}^d is defined to be $\hat{\mathbf{X}} = U_A S_A^{1/2}$, where*

$$|A| = (A^\top A)^{1/2} = \begin{bmatrix} U_A & \tilde{U}_A \end{bmatrix} \begin{bmatrix} S_A \oplus \tilde{S}_A \end{bmatrix} \begin{bmatrix} U_A & \tilde{U}_A \end{bmatrix}^\top,$$

is the spectral decomposition of $|A|$, $S_A \in \mathbb{R}^{d \times d}$ is the diagonal matrix with the d largest eigenvalues of $|A|$, and $U_A \in \mathbb{R}^{n \times d}$ the corresponding matrix of the d -largest eigenvectors.

Now, if we define $\hat{\mathbf{X}} = U_A S_A^{1/2}$, where S_A is the diagonal matrix of the top d eigenvalues of $(A^\top A)^{1/2}$, sorted by magnitude, and the columns of U_A are the associated unit eigenvectors, then [44] and [32] establish that, under assumptions on the spectrum of P , the rows $\hat{\mathbf{X}}$ are consistent estimates of the latent positions $\{\mathbf{X}_i\}$ (up to orthogonal rotation). Further, in [4], it is shown that under the RDPG, the (suitably-scaled) ASE of the adjacency matrix converges in distribution to a Gaussian mixture.

The utility of the ASE in single graph inference points us to a natural test statistic for determining whether two random dot product graphs have the same latent positions. Namely, we can perform Procrustes alignment of two graphs' embeddings [45]. Specifically, let $A^{(1)}$ and $A^{(2)}$ be the adjacency matrices of two random dot product graphs on the same vertex set, with vertices aligned so that vertex i in $A^{(1)}$ can be sensibly identified with vertex i in $A^{(2)}$ for all $i \in [n]$. Letting \hat{X} and \hat{Y} be the respective adjacency spectral embeddings of these two graphs, if the two graphs have the same generating P matrices, then it is reasonable to surmise that the Procrustes distance

$$\min_{\mathbf{W} \in \mathcal{O}^{d \times d}} \|\hat{X} - \hat{Y} \mathbf{W}\|_F, \quad (4)$$

will be small. In [45], the authors show that a scaled version of the Procrustes distance in (4) provides a valid and consistent test for the equality of latent positions for pairs of graphs. Unfortunately, the fact that a Procrustes minimization must be performed both complicates the test statistic and compromises its power.

The Procrustes alignment is necessary, though, because these two embeddings may well inhabit different d -dimensional subspaces of \mathbb{R}^n . An alternative approach is to consider jointly embedding a collection of random graphs into the *same* subspace, which is the topic of [26] and which we extend here. To start, we first define a model for an m -fold collection of d -dimensional random graphs.

Definition 2.4 (Joint Random Dot Product Graph). *Let F be a distribution on a set $\mathcal{X} \in \mathbb{R}^d$ satisfying $\langle x, x' \rangle \in [0, 1]$ for all $x, x' \in \mathcal{X}$. Let $X_1, X_2, \dots, X_n \sim F$ be i.i.d. random variables distributed via F , and let $P = \mathbf{X}\mathbf{X}^T$, where $\mathbf{X} = [X_1^T | X_2^T | \dots | X_n^T]^T \in \mathbb{R}^{n \times d}$. The random graphs $(A^{(1)}, A^{(2)}, \dots, A^{(m)})$ are distributed as a Joint Random Dot Product Graph (abbreviated JRDPG), written*

$$(A^{(1)}, A^{(2)}, \dots, A^{(m)}, \mathbf{X}) \sim \text{JRDPG}(F, n, m)$$

if marginally each $(A^{(i)}, \mathbf{X}) \sim \text{RDPG}(F, n)$ and conditioned on \mathbf{X} the $A^{(i)}$ are independent with distribution given by Eq. (1).

In the above definition, once the latent position matrix is generated, the m independent random graphs with respective adjacency matrices A_1, \dots, A_m all have the same connection probability matrix P . That is, $\mathbb{E}(A^{(i)} | \mathbf{X}) = P$ for all i . This is a direct graph-analogue of i.i.d Euclidean data from the same generating distribution, and given that we have *multiple* independent adjacency matrices from the same distribution, it is plausible that a latent position inference procedure using all the $A^{(i)}$ matrices is superior to an inference procedure that depends on a single $A^{(i)}$. In addition, since individual graph embeddings cannot be compared without Procrustes alignments, a joint embedding procedure that eliminates post-hoc pairwise alignments can be particularly useful. In [26], the authors build a spectral embedding of an $mn \times mn$ matrix M from the A_i matrices by placing each $A^{(i)}$ on the main block-diagonal and, on the (i, j) -th off-diagonal block, the average $\frac{A^{(i)} + A^{(j)}}{2}$. That is, for, say the $m = 2$ case, the matrix M is

$$M = \begin{bmatrix} A^{(1)} & \frac{A^{(1)} + A^{(2)}}{2} \\ \frac{A^{(1)} + A^{(2)}}{2} & A^{(2)} \end{bmatrix}, \quad (5)$$

Observe that the expected value of M is the matrix

$$\mathbb{E}[M] = \begin{bmatrix} P & P \\ P & P \end{bmatrix}, \quad (6)$$

which is still a rank d matrix. As a consequence, a d -dimensional embedding of M can produce an m -fold collection of *correlated* estimates for the rows of the latent position matrix \mathbf{X} . This *joint* or *omnibus* spectral embedding, denoted *OMNI*, is defined as follows.

Definition 2.5 (Omnibus Spectral Embedding). *Let $A^{(1)}, A^{(2)}, \dots, A^{(m)}$ be a collection of m graphs each in \mathcal{G}_n . Define the omnibus matrix of $A^{(1)}, A^{(2)}, \dots, A^{(m)}$ to be the $mn \times mn$ matrix M defined via*

$$M = \begin{bmatrix} A^{(1)} & \frac{A^{(1)} + A^{(2)}}{2} & \frac{A^{(1)} + A^{(3)}}{2} & \dots & \frac{A^{(1)} + A^{(m)}}{2} \\ \frac{A^{(2)} + A^{(1)}}{2} & A^{(2)} & \frac{A^{(2)} + A^{(3)}}{2} & \dots & \frac{A^{(2)} + A^{(m)}}{2} \\ \frac{A^{(3)} + A^{(1)}}{2} & \frac{A^{(3)} + A^{(2)}}{2} & A^{(3)} & \dots & \frac{A^{(3)} + A^{(m)}}{2} \\ \vdots & \vdots & & \ddots & \vdots \\ \frac{A^{(m)} + A^{(1)}}{2} & \frac{A^{(m)} + A^{(2)}}{2} & \frac{A^{(m)} + A^{(3)}}{2} & \dots & A^{(m)} \end{bmatrix}.$$

The d -dimensional Omnibus Spectral Embedding of $A^{(1)}, A^{(2)}, \dots, A^{(m)}$ is then given by

$$\text{OMNI}(A^{(1)}, A^{(2)}, \dots, A^{(m)}, d) = \text{ASE}(M, d) = U_M S_M^{1/2},$$

where $\text{ASE}(M, d)$ is the d -dimensional adjacency spectral embedding of M ; that is, S_M is the diagonal matrix of the top d eigenvalues of M , and U_M the corresponding eigenvectors.

Note that the omnibus embedding is an $mn \times d$ -dimensional matrix. Each n -fold block of rows supplies an $n \times d$ matrix that can serve as a latent position estimate for the corresponding graph. That is, the s -th $n \times d$ block of the omnibus embedding, denoted $\hat{\mathbf{X}}^{(s)} = [U_M S_M^{1/2}]^s$, is an estimate for $\mathbf{X}^{(s)}$, the matrix of latent positions for the s -th graph.

In [26], it is shown that—in parallel to the same result for the ASE—when all graphs have the same underlying latent positions, the rows of the omnibus embedding provide simultaneously consistent estimation for the latent positions X_j , where $1 \leq j \leq n$. There are m such rows for each vertex j . In addition, [26] demonstrates that for fixed m , as $n \rightarrow \infty$, the distribution of any fixed k subcollection of the rows of the omnibus matrix, suitably scaled, converges in distribution to a mixture of Gaussians.

The omnibus embedding forces correlation across the estimated latent positions, and in return it obviates the need for Procrustes alignments between $n \times d$ matrices $\hat{\mathbf{X}}^l$ and $\hat{\mathbf{X}}^s$, where $1 \leq l \leq s \leq m$. With the omnibus embedding, an empirically useful test statistic for assessing latent position equality is simply the Frobenius norm $\|\hat{\mathbf{X}}^l - \hat{\mathbf{X}}^s\|_F$.

Quantifying the correlation induced by this joint embedding, and determining how it relates to the choice of block-matrix on the off-diagonal of M , is an important question. The classical omnibus matrix uses a simple pairwise average, chosen to balance the requirements of estimation accuracy (when all graphs have the same latent positions) with the need to retain discriminatory power in hypothesis testing (when some of the graphs have different latent positions). By analyzing precisely how the off-diagonal blocks can impact this correlation, we can describe how the omnibus embedding can be used to perform inference on collections of graphs that are not necessarily independent, or can replicate some desired correlation structure in spectral estimates.

3 Latent and induced correlation

Consider the task of embedding a pair of n -vertex correlated d -dimensional random dot product graphs, $(B^{(1)}, B^{(2)}, \mathbf{X}) \sim \text{RDGP}(F, n, \rho)$. Prior to the development of methods to jointly embed the networks, a common approach was to separately embed the two graphs into a common Euclidean space, and then align the networks via orthogonal Procrustes analysis [45]. Our motivating question was how to capture the effect of the correlation on the embedded pair. Before delving into the theoretical exposition, we first consider a simple, motivating example. Consider $n = 300$, $\rho \in \{0, 0.25, 0.5, 0.75, 1\}$ and F a mixture of point mass distributions defined via:

$$F = \frac{1}{2}\delta_{\xi_1} + \frac{1}{2}\delta_{\xi_2}, \tag{7}$$

where $\xi_1, \xi_2 \in \mathbb{R}^2$ satisfy

$$\begin{bmatrix} \xi_1 \\ \xi_2 \end{bmatrix} \begin{bmatrix} \xi_1 \\ \xi_2 \end{bmatrix}^T = \begin{bmatrix} 0.7 & 0.3 \\ 0.3 & 0.5 \end{bmatrix}$$

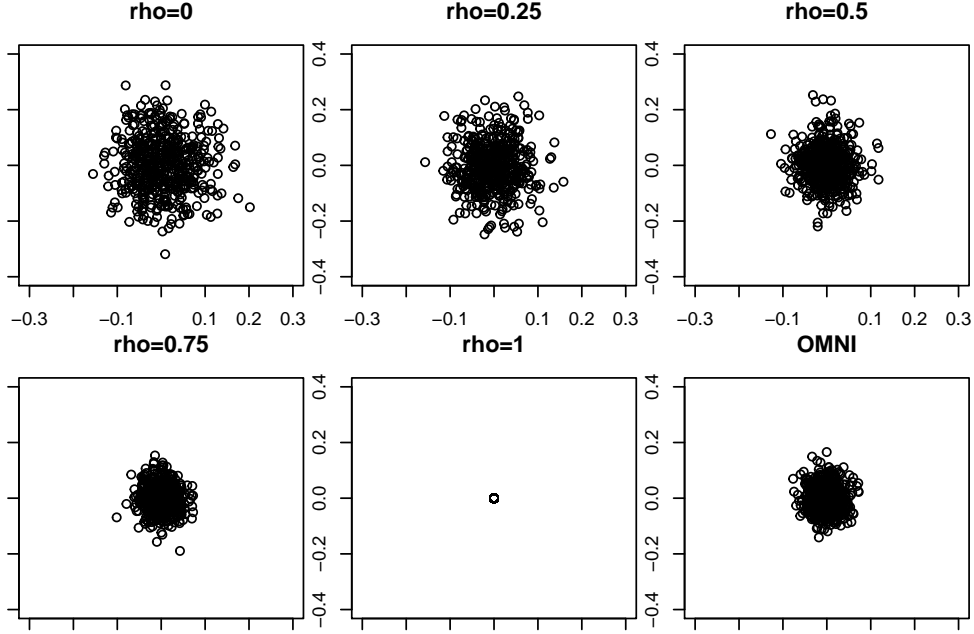


Figure 1: The effect of induced versus latent correlation in the embedded space. In panels 1–5 we plot, for various levels of ρ , the difference in the aligned estimates of X_1 from separately spectrally embedding $(B^{(1)}, B^{(2)}, \mathbf{X}) \sim \text{RDPG}(F, n, \rho)$ (where F has the form in Eq. (7)). In the sixth panel, we consider $(B^{(1)}, B^{(2)}, \mathbf{X}) \sim \text{JRDPG}(F, 300, 2)$, and plot the difference in the pair of estimates of $X_1 = \xi_1$ derived from the omnibus embedding. In all panels, the experiment was repeated $nMC = 500$ times.

(so that the RDPG’s drawn from F are examples of correlated *Stochastic Blockmodel* random graphs [23]). In order to better understand the role of the correlation in the embedded space, we separately spectrally embed each network, $\hat{\mathbf{X}}^{(1)} = \text{ASE}(B^{(1)}, 2)$ and $\hat{\mathbf{X}}^{(2)} = \text{ASE}(B^{(2)}, 2)$, and then align the networks via $\hat{\mathbf{X}}^{(1)}W^{(1)}$ and $\hat{\mathbf{X}}^{(2)}W^{(2)}$ where for each $k = 1, 2$,

$$W^{(k)} = \text{argmin}_{W \in \mathcal{O}_2} \|\hat{\mathbf{X}}^{(i)}W - \mathbf{X}\|_F.$$

In Figure 1, we plot $(\hat{\mathbf{X}}^{(1)}W^{(1)} - \hat{\mathbf{X}}^{(2)}W^{(2)})_1$ (i.e., the first row of $\hat{\mathbf{X}}^{(1)}W^{(1)} - \hat{\mathbf{X}}^{(2)}W^{(2)}$), the distance between the (aligned) estimates of $X_1 = \xi_1$ derived from the embeddings over a range of values of ρ ; note that in each panel the experiment is repeated $nMC = 500$ times. In the first five panels of the figure, we see the effect of increasing ρ on the difference, namely that the covariance of the difference is monotonically decreasing as ρ increases.

In the sixth panel of Figure 1 (again considering $nMC = 500$ Monte Carlo replicates), we consider the $\rho = 0$ (i.e., conditionally independent case), so that $(B^{(1)}, B^{(2)}, \mathbf{X}) \sim \text{JRDPG}(F, 300, 2)$. We consider the omnibus spectral embedding of $(B^{(1)}, B^{(2)})$, denoted $\hat{\mathbf{X}}_M = \text{OMNI}(B^{(1)}, B^{(2)}, 2)$, and plot the difference in the estimates of $X_1 = \xi_1$ derived from the omnibus embedding, namely $(\hat{\mathbf{X}}_M)_1 - (\hat{\mathbf{X}}_M)_{301}$. From the figure, we see that the correlation induced between the independent graphs in embedded space is (roughly) equivalent to the latent correlation between $\rho = 0.75$ correlated networks that have been separately embedded and aligned. In the next section, we will formalize this notion of induced versus

latent correlation, and we will see that, as the Figure suggests, OMNI does indeed induce correlation of level $\rho = 0.75$ across independent graphs in the embedded space.

3.1 Central limit theorems and correlation in the embedded space

Viewing $(B^{(1)}, B^{(2)}, \mathbf{X})$ as an element of the sequence

$$((B_n^{(1)}, B_n^{(2)}, \mathbf{X}_n))_{n=1}^\infty,$$

where for each $n \geq 1$, $(B_n^{(1)}, B_n^{(2)}, \mathbf{X}_n) \sim \text{RDPG}(F, n, \rho)$, the Central Limit Theorem paradigm established in [4] provides a path forward for rigorously understanding the effect, in the embedded space, of the edge-wise correlation across networks. Letting $\widehat{\mathbf{X}}_n^{(1)} = \text{ASE}(B_n^{(1)}, d)$ and $\widehat{\mathbf{X}}_n^{(2)} = \text{ASE}(B_n^{(2)}, d)$, Theorem 3.3 of [4] (in the form presented in Theorem 9 of [3]) implies that if $\Delta := \mathbb{E}[X_1 X_1^T]$ is rank d , then there exists a sequence of orthogonal d -by- d matrices $(\tilde{W}_n)_{n=1}^\infty$ such that for all $z \in \mathbb{R}^d$ and for any fixed index i , and for each $k = 1, 2$,

$$\lim_{n \rightarrow \infty} \mathbb{P} \left[n^{1/2} \left(\widehat{\mathbf{X}}_n^{(k)} \tilde{W}_n - \mathbf{X}_n \right)_i \leq z \right] = \int_{\text{supp } F} \Phi(z, \Sigma(x)) dF(x),$$

where

$$\Sigma(x) := \Delta^{-1} \mathbb{E} \left[(x^T X_1 - (x^T X_1)^2) X_1 X_1^T \right] \Delta^{-1}; \quad (8)$$

$\Phi(\cdot, \Sigma)$ denote the cdf of a (multivariate) Gaussian with mean zero and covariance matrix Σ , and $(\widehat{\mathbf{X}}_n \tilde{W}_n - \mathbf{X}_n)_i$ denotes the i -th row of $\widehat{\mathbf{X}}_n \tilde{W}_n - \mathbf{X}_n$. Combining the above central limit theorems for $\widehat{\mathbf{X}}_n^{(1)}$ and $\widehat{\mathbf{X}}_n^{(2)}$, we have the following theorem (proven in Section A.1).

Theorem 1. *Let $\rho \in (0, 1)$ be fixed. Let F be a distribution on a set $\mathcal{X} \subset \mathbb{R}^d$, where $\{x, x'\} \in [0, 1]$ for all $x, x' \in \mathcal{X}$, and assume that $\Delta := \mathbb{E}[X_1 X_1^T]$ is rank d . Let $(B_n^{(1)}, B_n^{(2)}, \mathbf{X}_n) \sim \text{RDPG}(F, n, \rho)$, be a sequence of adjacency matrices and associated latent positions, where for each $n \geq 1$ the rows of \mathbf{X}_n are i.i.d. distributed according to F . Letting $\widehat{\mathbf{X}}_n^{(1)} = \text{ASE}(B_n^{(1)}, d)$ and $\widehat{\mathbf{X}}_n^{(2)} = \text{ASE}(B_n^{(2)}, d)$, there exists sequences of orthogonal d -by- d matrices $(W_n^{(1)})_{n=1}^\infty$, $(W_n^{(2)})_{n=1}^\infty$ such that for all $z \in \mathbb{R}^d$ and for any fixed index i ,*

$$\lim_{n \rightarrow \infty} \mathbb{P} \left[n^{1/2} \left(\widehat{\mathbf{X}}_n^{(1)} W_n^{(1)} - \widehat{\mathbf{X}}_n^{(2)} W_n^{(2)} \right)_i \leq z \right] = \int_{\text{supp } F} \Phi \left(z, \tilde{\Sigma}(x, \rho) \right) dF(x), \quad (9)$$

where $\tilde{\Sigma}(x, \rho) = 2(1 - \rho)\Sigma(x)$.

From Theorem 1, we see that the effect of the correlation ρ in the embedding space is to introduce a dampening factor of $(1 - \rho)$ into the asymptotic limiting covariance (see Figure 1). This is entirely reasonable (indeed, consider Y_1, Y_2 to be ρ correlated $\text{Norm}(\mu, \sigma^2)$ random variables, then $Y_1 - Y_2 \sim \text{Norm}(0, 2(1 - \rho)\sigma^2)$ as desired), and no extraneous correlation is introduced (at least in the limit) by separately embedding the networks and aligning the embeddings via $(W_n^{(k)})_{n=1}^\infty$ for $k = 1, 2$. Joint embedding procedures like the omnibus method, in forgoing the Procrustes rotations, will induce correlation across even independent networks. To understand this better, we consider the omnibus central limit theorem framework of [26] to derive the following theorem (whose proof is an immediate consequence of Theorem 4).

Theorem 2. Let F be a distribution on a set $\mathcal{X} \subset \mathbb{R}^d$, where $\{x, x'\} \in [0, 1]$ for all $x, x' \in \mathcal{X}$, and assume that $\Delta := \mathbb{E}[X_1 X_1^T]$ is rank d . Let $(A_n^{(1)}, A_n^{(2)}, \dots, A_n^{(m)}, \mathbf{X}_n) \sim \text{JRDPG}(F, n, m)$ be a sequence of JRDPG random graphs, and for each $n \geq 1$, let M_n denote the omnibus matrix as in Definition 2.5 and $\hat{\mathbf{X}}_{M_n} = \text{ASE}(M_n, d)$. Consider fixed indices i and $s_1, s_2 \in [m]$ and set $h_1 = n(s_1 - 1) + i$, and $h_2 = n(s_2 - 1) + i$. Then there exists a sequence of orthogonal matrices $(\tilde{W}_n)_{n=1}^\infty$ such that

$$\lim_{n \rightarrow \infty} \mathbb{P} \left[n^{1/2} \left[\left(\hat{\mathbf{X}}_{M_n} \tilde{W}_n \right)_{h_1} - \left(\hat{\mathbf{X}}_{M_n} \tilde{W}_n \right)_{h_2} \right] \leq z \right] = \int_{\text{supp } F} \Phi(z, \tilde{\Sigma}(x, 3/4)) dF(x). \quad (10)$$

Unpacking Theorem 2, first note that $(\hat{\mathbf{X}}_{M_n})_{h_1}$ and $(\hat{\mathbf{X}}_{M_n})_{h_2}$ represent the estimates of X_i derived from $A^{(s_1)}$ and $A^{(s_2)}$ by the omnibus embedding paradigm. In light of Theorem 1, the induced correlation in OMNI can be understood in the context of the limiting covariance of the difference of a pair of estimates for the same underlying latent position. Comparing Eqs. (9) and (10), we see that OMNI effectively induces a correlation of level $\rho = 3/4$ uniformly across embedded network pairs. This correlation is independent of m and the particular indices s_1 and s_2 chosen, suggesting that OMNI is not ideal for embedding temporal sequences of networks that exhibit a change point or anomaly. Indeed, OMNI is unable to induce more complex correlation structures amongst the embedded $A^{(i)}$, and the OMNI embedding is a poor surrogate for edge-wise correlated networks that are embedded separately and then aligned. We demonstrate in the next section that we can partially remedy these issues by considering more general structures in the OMNI matrix M .

4 Generalized omnibus embeddings

The consistency and asymptotic normality of the classical omnibus embedding rest on a few defining model assumptions: first,

$$\mathbb{E}(M_n) = \tilde{P} := J_m \otimes P,$$

and second, in the i -th block-row of M_n , the weight put on A_i (which is equal to $1 + (m-1)/2$) is strictly greater than the weight put on any A_j for $j \neq i$ (as each of these is $1/2$). The low-rank RDPG structure of $\mathbb{E}(M_n) = \tilde{P}$ allows us to use random matrix concentration results to prove that the scaled eigenvectors of M_n are tightly concentrated about the scaled eigenvectors of \tilde{P} which, up to a possible rotation, are equal to $\mathbf{Z} := \tilde{\mathbf{I}}_m \otimes \mathbf{X}$. The weights in block-row i being maximized for A_i ensures that the i -th block in $\text{ASE}(M_n, d)$ corresponds to the embedding of A_i , which is essential for subsequent inference (e.g., hypothesis testing [13]) in the omnibus setting.

It is natural to ask if, subject to the above conditions, we can generalize the omnibus structure to permit more esoteric induced correlation in the embedded space. This motivates the following definition of the generalized omnibus matrix. Let F be a distribution on a set $\mathcal{X} \subset \mathbb{R}^d$, where $\{x, x'\} \in [0, 1]$ for all $x, x' \in \mathcal{X}$. Suppose that $(A^{(1)}, A^{(2)}, \dots, A^{(m)}, \mathbf{X}) \sim \text{JRDPG}(F, n, m)$, and let $k \in [m]$. The convex hull of $A^{(1)}, A^{(2)}, \dots, A^{(m)}$ is denoted via

$$\mathcal{A}_m = \left\{ \sum_{i=1}^m c_i A^{(i)} \in \mathbb{R}^{n \times n} \mid \text{with } c_i \geq 0 \text{ for all } i \in [m] \text{ and } \sum_{i=1}^m c_i = 1 \right\}.$$

Definition 4.1 (Generalized Omnibus Matrix). Consider $\mathfrak{M} \in \mathbb{R}^{mn \times mn}$, a generalized version of the omnibus M of Definition 2.5 defined as follows. \mathfrak{M} is a block matrix satisfying the following assumptions:

1. Each block entry $\mathfrak{M}^{(i,j)} \in \mathbb{R}^{n \times n}$, $i, j \in [m]$ is an element of \mathcal{A}_m ; in the sequel, we will write $\mathfrak{M}^{(i,j)} = \sum_{\ell=1}^m c_\ell^{(i,j)} A^{(\ell)}$
2. For each block row $i \in [m]$ of \mathfrak{M} , the cumulative weight of $A^{(i)}$ is greater than the cumulative weight of the rest of the $A^{(\ell)}$, $\ell \neq i$; i.e., for $\ell \neq i$

$$\sum_j c_\ell^{(i,j)} < \sum_j c_i^{(i,j)}.$$

3. \mathfrak{M} is symmetric.

Such a block matrix satisfying assumptions 1-3 above will be referred to as a Generalized Omnibus Matrix.

IF \mathfrak{M} is a Generalized Omnibus Matrix, then each block of \mathfrak{M} being an element of \mathcal{A}_m ensures that $\mathbb{E}(\mathfrak{M}) = \tilde{P}$, and setting $\alpha(i, \ell) = \sum_j c_\ell^{(i,j)}$ to be the weight put on A_ℓ in the i -th block-row of \mathfrak{M} , assumption 2 above ensures that for each $i \in [m]$,

$$\alpha(i, \ell) < \alpha(i, i) \quad \text{for all } \ell \neq i. \quad (11)$$

Because \mathfrak{M} (i.e., $\mathbb{E}(\mathfrak{M}) = \tilde{P}$) is unbiased and low-rank, we can appropriately modify matrix concentration and perturbation results for the scaled eigenvectors of \mathfrak{M} , and we can establish that the rows of $\text{ASE}(M_n, d)$ consistently estimate the associated rows of \mathbf{Z} and the associated residual errors satisfy a distributional central limit theorem (whose proof can be found in Appendix A.4).

Theorem 3. Let F be a distribution on a set $\mathcal{X} \subset \mathbb{R}^d$, where $\{x, x'\} \in [0, 1]$ for all $x, x' \in \mathcal{X}$, and assume that $\Delta := \mathbb{E}[X_1 X_1^T]$ is rank d . Let $(A_n^{(1)}, A_n^{(2)}, \dots, A_n^{(m)}, \mathbf{X}_n) \sim \text{JRDPG}(F, n, m)$ be a sequence of JRDPG random graphs, and let $\mathbf{Z}_n = [\mathbf{X}_n^T | \mathbf{X}_n^T] \dots [\mathbf{X}_n^T]^T \in \mathbb{R}^{mn \times d}$. Further, for each $n \geq 1$, let \mathfrak{M}_n denote the generalized omnibus matrix as in Definition 4.1 and $\hat{\mathbf{X}}_{\mathfrak{M}_n} = \text{ASE}(\mathfrak{M}_n, d)$. If $h = n(s-1) + i$, for fixed $i \in [n]$, $s \in [m]$, then there exists a sequence of orthogonal matrices $\{\mathcal{R}_n\}_n$ such that

$$\lim_{n \rightarrow \infty} \mathbb{P} \left[n^{1/2} \left(\hat{\mathbf{X}}_{\mathfrak{M}_n} \mathcal{R}_n - \mathbf{Z}_n \right)_h \leq z \right] = \int_{\text{supp} F} \Phi(z, \check{\Sigma}(x)) dF(x),$$

where

$$\check{\Sigma}(x) = \frac{1}{m^2} \left(\sum_{\ell=1}^m \alpha^2(s, \ell) \right) \Delta^{-1} \mathbb{E} \left[(x^T X_j - (x^T X_j)^2) X_j X_j^T \right] \Delta^{-1} = \frac{1}{m^2} \left(\sum_{\ell=1}^m \alpha^2(s, \ell) \right) \Sigma(x).$$

Since $\alpha(s, \ell) := \sum_{t=1}^m c_\ell^{(s,t)}$, the coefficient in the matrix $\check{\Sigma}(x)$ can be written in terms of c_ℓ 's, i.e.,

$$\check{\Sigma}(x) = \frac{1}{m^2} \sum_{\ell=1}^m \left(\sum_{t=1}^m (c_\ell^{(s,t)})^2 + 2 \sum_{t_1 < t_2} c_\ell^{(s,t_1)} c_\ell^{(s,t_2)} \right) \Sigma(x) \quad (12)$$

Under the JRDPG model, Eq. (12) reveals precisely the effect of a given omnibus matrix structure on the corresponding covariance matrices of the latent positions, $\check{\Sigma}(X_i)$. As an example, in the classical omnibus setting of [26],

$$c_\ell^{(i,j)} = \begin{cases} 1 & \text{if } i = j = \ell \\ 1/2 & \text{if } i \neq j, \text{ and } \ell \in \{i, j\} \\ 0 & \text{else,} \end{cases}$$

and so

$$\alpha(s, \ell) = \begin{cases} 1 + (m-1)/2 & \text{if } s = \ell \\ 1/2 & \text{else.} \end{cases}$$

The associated coefficient of $\Sigma(x)$ in $\check{\Sigma}(x)$ is then

$$\begin{aligned} \frac{1}{m^2} \left(\sum_{\ell=1}^m \alpha^2(s, \ell) \right) &= \frac{1}{m^2} ((m-1)/4 + (1 + (m-1)/2)^2) \\ &= \frac{1}{4m^2} (m^2 + 3m) \\ &= \frac{m+3}{4m}, \end{aligned}$$

which (of course) agrees with the covariance structure computed in [26, Theorem 1].

Moving beyond the classical case, the following examples of generalized omnibus structures highlight the impact the structure of \mathfrak{M} has on the limiting covariance (and hence on the limiting induced correlation; see Theorem 3).

Example 1. Total Average Omnibus In the total average case, letting

$$\bar{A} = \frac{A^{(1)} + A^{(2)} + \dots + A^{(m)}}{m},$$

we define the generalized omnibus matrix \mathfrak{M}_A via

$$\mathfrak{M}_A = \begin{bmatrix} A^{(1)} & \bar{A} & \dots & \bar{A} \\ \bar{A} & A^{(2)} & \dots & \bar{A} \\ \vdots & \vdots & \ddots & \vdots \\ \bar{A} & \bar{A} & \dots & A^{(m)} \end{bmatrix}.$$

In this example,

$$c_\ell^{(i,j)} = \begin{cases} 1 & \text{if } i = j = \ell \\ 1/m & \text{else,} \end{cases}$$

and so

$$\alpha(s, \ell) = \begin{cases} 1 + (m-1)/m & \text{if } s = \ell \\ (m-1)/m & \text{else.} \end{cases}$$

The associated coefficient of $\Sigma(x)$ in $\check{\Sigma}(x)$ is then

$$\begin{aligned} \frac{1}{m^2} \left(\sum_{\ell=1}^m \alpha^2(s, \ell) \right) &= \frac{1}{m^2} \left((m-1)^3/m^2 + (1 + (m-1)/m)^2 \right) \\ &= \frac{m^2 + m - 1}{m^3}. \end{aligned}$$

In the classical setting, for large m , the limiting covariance is approximately $\Sigma(x)/4$, and is not degenerate; in the total average omnibus setting for large m , the limiting covariance is approximately $\Sigma(x)/m \approx 0$. This is sensible heuristically, as in that setting, we are effectively embedding $J_m \otimes \bar{A} \approx \bar{P}$, and the correct scaling of the residuals would ideally be \sqrt{nm} rather than \sqrt{n} .

Example 2. Weighted Pairwise Average Omnibus In the classical omnibus setting, we have that

$$\mathfrak{M}^{(i,j)} = \frac{A^{(i)} + A^{(j)}}{2},$$

and all matrices are effectively weighted equally in the omnibus matrix. This is sensible if all $A^{(i)}$ are i.i.d., but is, perhaps, less ideal in the setting where the networks are noisily observed with the level of noise varying in $i \in [m]$. In that setting, the *Weighted* Pairwise Average Omnibus matrix defined via

$$\mathfrak{M}_W = \begin{bmatrix} A^{(1)} & \frac{w_1 A^{(1)} + w_2 A^{(2)}}{w_1 + w_2} & \frac{w_1 A^{(1)} + w_3 A^{(3)}}{w_1 + w_3} & \dots & \frac{w_1 A^{(1)} + w_m A^{(m)}}{w_1 + w_m} \\ \frac{w_2 A^{(2)} + w_1 A^{(1)}}{w_2 + w_1} & A^{(2)} & \frac{w_2 A^{(2)} + w_3 A^{(3)}}{w_2 + w_3} & \dots & \frac{w_2 A^{(2)} + w_m A^{(m)}}{w_2 + w_m} \\ \frac{w_3 A^{(3)} + w_1 A^{(1)}}{w_3 + w_1} & \frac{w_3 A^{(3)} + w_2 A^{(2)}}{w_3 + w_2} & A^{(3)} & \dots & \frac{w_3 A^{(3)} + w_m A^{(m)}}{w_3 + w_m} \\ \vdots & \vdots & \vdots & \ddots & \vdots \\ \frac{w_m A^{(m)} + w_1 A^{(1)}}{w_m + w_1} & \frac{w_m A^{(m)} + w_2 A^{(2)}}{w_m + w_2} & \frac{w_m A^{(m)} + w_3 A^{(3)}}{w_m + w_3} & \dots & A^{(m)} \end{bmatrix}$$

may be more appropriate. In this case, the block entries of the omnibus matrix are defined via

$$\mathfrak{M}_W^{(i,j)} = \frac{w_i A^{(i)} + w_j A^{(j)}}{w_i + w_j}$$

with weights $w_i > 0$ $i, j \in [m]$. In this example,

$$c_\ell^{(i,j)} = \begin{cases} 1 & \text{if } i = j = \ell \\ \frac{w_\ell}{w_\ell + w_j} & \text{if } \ell = i \neq j \\ \frac{w_\ell}{w_\ell + w_i} & \text{if } \ell = j \neq i \\ 0 & \text{else,} \end{cases}$$

and so

$$\alpha(s, \ell) = \begin{cases} 1 + \sum_{k \neq s} \frac{w_s}{w_s + w_k} & \text{if } s = \ell \\ \frac{w_\ell}{w_\ell + w_s} & \text{else.} \end{cases}$$

As (if each $w_i > 0$) $\alpha(s, \ell) < 1$ for $\ell \neq s$, we immediately have that $\alpha(s, s) > \alpha(s, \ell)$ for $\ell \neq s$. While the associated coefficient of $\Sigma(x)$ in $\check{\Sigma}(x)$ is not easily expressed in general, specific examples can nonetheless be instructive. Consider the setting where $w_1 = w$ and $w_i = 1$ for all $i \neq 1$. Considering $s = 1$ in Theorem 3 provides that the associated coefficient of $\Sigma(x)$ in $\check{\Sigma}(x)$ is

$$\begin{aligned} \frac{1}{m^2} \left(\sum_{\ell=1}^m \alpha^2(s, \ell) \right) &= \frac{1}{m^2} \left((m-1) \frac{1}{(1+w)^2} + (1 + (m-1)w/(1+w))^2 \right) \\ &= \frac{m-1 + (1+mw)^2}{m^2(1+w)^2}. \end{aligned}$$

If w is large, then this coefficient is approximately equal to 1, which is the limiting covariance achieved by embedding $A^{(1)}$ separately. This will be further explained in the context of limiting induced correlation in the next section. If w is small, then this coefficient is of the order $1/m$, and increasing the number of graphs in the embedding results in a degenerate limiting covariance for the underweighted network in the embedded space.

4.1 Limiting induced correlation

In the generalized omnibus embedding, similar to in the classical setting, we can precisely compute the limiting induced correlation between estimates of the same latent position in the embedded space. To wit, we have the following Theorem whose proof can be found in Appendix B.

Theorem 4. *With notation and assumptions as in Theorem 3, consider fixed indices $i \in [n]$ and $s, s_1, s_2 \in [m]$ and set $h = n(s-1) + i$, $h_1 = n(s_1-1) + i$, $h_2 = n(s_2-1) + i$. Denote the estimated latent position from graph $A^{(s)}$ of the hidden latent position X_i as $(\hat{\mathbf{X}}_{\mathfrak{M}_n})_h = (ASE(\mathfrak{M}_n, d))_h$. There exists a sequence of orthogonal matrices $(\mathcal{R}_n)_{n=1}^\infty$ such that for all $z \in \mathbb{R}^d$, we have that*

$$\lim_{n \rightarrow \infty} \mathbb{P} \left[n^{1/2} \left((\hat{\mathbf{X}}_{\mathfrak{M}_n})_{h_1} - (\hat{\mathbf{X}}_{\mathfrak{M}_n})_{h_2} \right) \mathcal{R}_n \leq z \right] = \int_{\text{supp } F} \Phi \left(z, \tilde{\Sigma}(x, \rho(s_1, s_2)) \right) dF(x), \quad (13)$$

where $\rho(s_1, s_2)$ is given by

$$\rho(s_1, s_2) = 1 - \frac{\sum_{\ell=1}^m (\alpha(s_1, \ell) - \alpha(s_2, \ell))^2}{2m^2}. \quad (14)$$

Before considering the more exotic examples considered above, recall that in the classical omnibus embedding setting, we have that

$$\alpha(s, \ell) = \begin{cases} 1 + (m-1)/2 & \text{if } s = \ell \\ 1/2 & \text{otherwise} \end{cases}$$

Plugging this into Eq. (14), we see that $\rho(s_1, s_2) = 3/4$ for all distinct $s_1, s_2 \in [m]$, and Theorem 2 is thus proven.

Example 1 con. In the total average case, we have that

$$\begin{aligned}\rho(s_1, s_2) &= 1 - \frac{\sum_{\ell=1}^m (\alpha(s_1, \ell) - \alpha(s_2, \ell))^2}{2m^2} \\ &= 1 - \frac{2}{2m^2} = 1 - \frac{1}{m^2}.\end{aligned}$$

This is sensible, as for large m we have that $\mathfrak{M}_A \approx J_m \otimes \bar{A}$ and the embedding of each $A^{(i)}$ is effectively equivalent to repeatedly embedding \bar{A} , yielding the large m correlation approximately equal to 1. Note also that this induced correlation is independent of the particular indices s_1 and s_2 , and also when $m = 2$, the induced correlation from the total average case coincides with the pairwise (unweighted) average case (i.e., the matrix structure as in Definition 2.5). However, the covariance matrix $\check{\Sigma}$ depends on m in the \mathfrak{M}_A setting, and for $m \geq 3$, the correlation induced by \mathfrak{M}_A is always greater than the correlation induced by the classical M .

Example 2 con. In the weighted average setting, the limiting induced correlation for the (scaled) row difference in Theorem 4 is given by

$$\begin{aligned}\rho(s_1, s_2) &= 1 - \frac{\sum_{\ell=1}^m (\alpha(s_1, \ell) - \alpha(s_2, \ell))^2}{2m^2} \\ &= 1 - \frac{a_{1,2}^2 + a_{2,1}^2 + (w_{s_1} - w_{s_2})^2 \sum_{\ell \neq s_1, s_2} \frac{w_\ell^2}{(w_{s_1} + w_\ell)^2 (w_{s_2} + w_\ell)^2}}{2m^2}\end{aligned}\tag{15}$$

where for $i, j \in [m]$,

$$a_{i,j} := 1 + \sum_{\ell \neq s_i, s_j} \frac{w_{s_i}}{w_\ell + w_{s_i}}.$$

Setting different values for the weights w_i , different block matrix structures are created which can exploit the relationship between the correlation of two estimates with the structure of the (weighted) omnibus matrix \mathfrak{M}_W . For instance, letting $w_{s_1} = w_{s_2}$, we have that $a_{1,2} = a_{2,1}$ and the limiting induced correlation is equal to

$$\rho(s_1, s_2) = 1 - \left(\frac{a_{1,2}}{m} \right)^2.$$

In the classical omnibus setting (where all $w_i = 1/2$) this further reduces to $\rho(s_1, s_2) = 3/4$, as, in this setting, $a_{i,j} = m/2$ for all $i, j \in [m]$.

Figure 2 further highlights this relationship between the matrix structure of \mathfrak{M}_W and the limiting covariance for the weighted pairwise average case. In this example, we set $m = 10$ and we set $w_{s_1} = w_{s_2} = 1$ (left panel) or $w_{s_1} = w_{s_2} = 10$ (right panel). The remainder of the weights, w_i $i \neq s_1, s_2$, are set to be equal, taking values in the interval $[0, 10]$. In this case,

$$a_{1,2} = \begin{cases} 1 + \frac{8}{1+w} & \text{left panel} \\ 1 + \frac{80}{10+w} & \text{right panel} \end{cases}$$

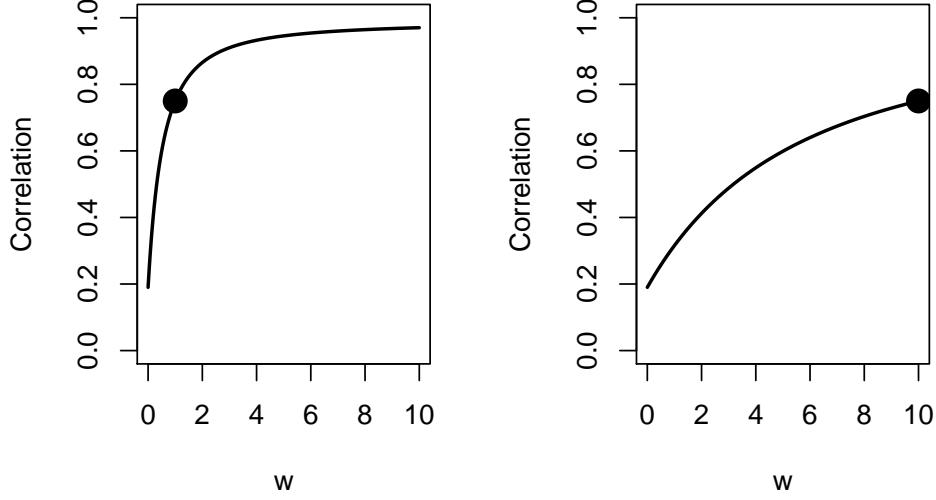


Figure 2: The number of graphs is $m = 10$. The plots illustrate the correlation $\rho(s_1, s_2)$ between estimates of the same true latent position across different values of the weights w_i , where $w_i = w_j$ for all $i, j \neq s_1, s_2$. Left panel: The limiting correlation between the estimated latent positions of the graphs $A^{(s_1)}$, $A^{(s_2)}$ when $w_{s_1} = w_{s_2} = 1$, and the black dot corresponds to the classical omnibus ([26]) case. Right panel: The limiting correlation between the estimated latent positions of the graphs $A^{(s_1)}$, $A^{(s_2)}$ when $w_{s_1} = w_{s_2} = 10$, and the black dot corresponds to the classical omnibus ([26]) case.

and

$$\rho(s_1, s_2) = \begin{cases} 1 - \left(\frac{9+w}{10(1+w)} \right)^2 & \text{left panel} \\ 1 - \left(\frac{90+w}{10(10+w)} \right)^2 & \text{right panel} \end{cases}$$

In each panel of Figure 2, we plot $\rho(s_1, s_2)$ as a function of w_i $i \neq s_1, s_2$, and we see that as the weights w_i , $i \neq s_1, s_2$ are decreasing, the correlation $\rho(s_1, s_2)$ decreases towards 0.19 as well (i.e., in the limit, the embedded estimates derived from $A^{(s_1)}$ and $A^{(s_2)}$ are “less” dependent on each other). On the contrary, as the weights w_i , $i \neq s_1, s_2$ are increasing, the correlation $\rho(s_1, s_2)$ increases (towards 1 in the $w_{s_1} = w_{s_2} = 1$ setting, and towards 0.75 in the $w_{s_1} = w_{s_2} = 10$ setting). Indeed, the driving force behind the limiting induced correlation between $A^{(s_1)}$ and $A^{(s_2)}$ is the cumulative weights of the other $A^{(i)}$ for $i \neq s_1, s_2$. If these weights are high, then the relative contribution to block-row s_1 (resp., s_2) by $A^{(s_1)}$ (resp., $A^{(s_2)}$) is small when compared to the cumulative effect of the other networks, and this masks the signal corresponding to $A^{(s_1)}$ (resp., $A^{(s_2)}$) in the s_1 -th (resp., s_2 -th) block of the embedding. If, however, the weights of the $A^{(i)}$ for $i \neq s_1, s_2$ are low, then the relative contribution to block-row s_1 (resp., s_2) by $A^{(s_1)}$ (resp., $A^{(s_2)}$) is large when compared to the cumulative effect of the other networks, and this has the effect of de-correlating $A^{(s_1)}$ and

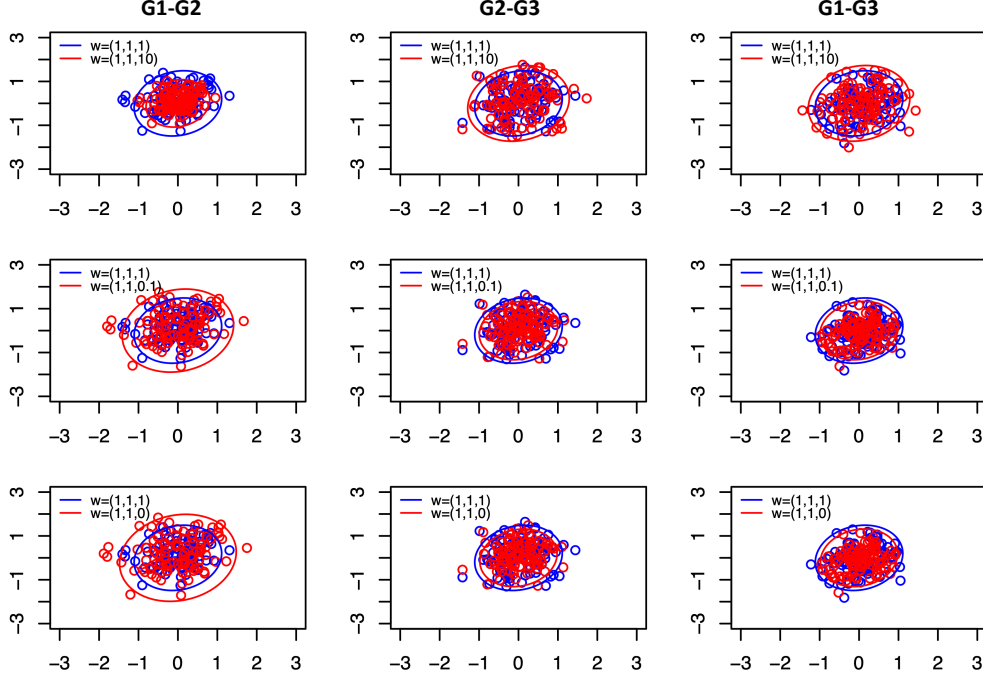


Figure 3: We consider $(A^{(1)}, A^{(2)}, A^{(3)}, \mathbf{X}) \sim \text{JRDPG}(F, 300, 3)$, and plot the difference in the pair of estimates of $X_1 = \xi_1$ derived from the omnibus embedding. Each column panel corresponds to a different pair of estimates, and each row panel corresponds to a different weighted omnibus matrix \mathfrak{M} created by the weight vectors $(1, 1, 10)$, $(1, 1, .1)$, $(1, 1, 0)$ (resp. top, middle, bottom). Each panel has estimates derived from two different omnibus embeddings, namely $\text{ASE}(M_0, 2)$ and $\text{ASE}(\mathfrak{M}, 2)$ (resp. blue and red points), and the experiment was repeated $nMC = 100$ times.

$A^{(s_2)}$.

We are also interested in showcasing how different assigned weights in the weighted pairwise average case affect the scaled difference between two estimates and their limiting covariance structure. To investigate this relation, we simulate three 300-vertex random undirected graphs $A^{(1)}, A^{(2)}, A^{(3)}$ via the JRDPG model from Definition 2.4 (i.e., $(A^{(1)}, A^{(2)}, A^{(3)}, \mathbf{X}) \sim \text{JRDPG}(F, 300, 3)$) with underlying distribution F be a mixture of point mass distributions defined via:

$$F = \frac{1}{2}\delta_{\xi_1} + \frac{1}{2}\delta_{\xi_2},$$

where $\xi_1, \xi_2 \in \mathbb{R}^2$ satisfy

$$\begin{bmatrix} \xi_1 \\ \xi_2 \end{bmatrix} \begin{bmatrix} \xi_1 \\ \xi_2 \end{bmatrix}^T = \begin{bmatrix} 0.7 & 0.2 \\ 0.2 & 0.7 \end{bmatrix} = P$$

Marginally, each graph is generated from the *Stochastic Blockmodel* with $K = 2$ communities and block probability matrix P . Further, we consider the weighted average omnibus matrices $\mathfrak{M} \in \mathbb{R}^{900 \times 900}$, created by the weight vectors

$$(w_1, w_2, w_3) \in \{(1, 1, 1), (1, 1, 10), (1, 1, .1), (1, 1, 0)\}.$$

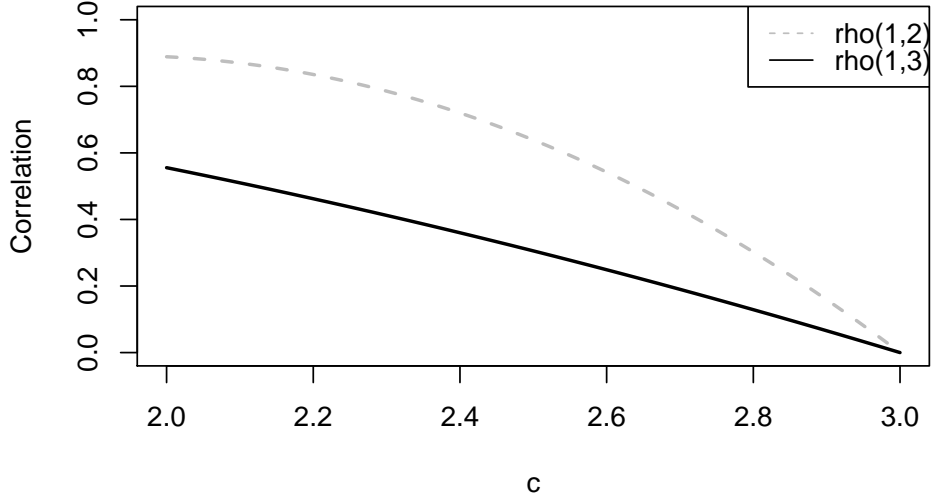


Figure 4: Correlation values for the α in Eq. (16) plotted as a function of $c \in (2, 3]$.

Letting $\hat{\mathbf{X}}_{\mathfrak{M}} = ASE(\mathfrak{M}, 2)$, in Figure 3 we plot the scaled differences between two estimates of $X_1 = \xi_1$ derived from the omnibus embedding, namely

$$\begin{aligned} & \sqrt{n} \left((\hat{\mathbf{X}}_{\mathfrak{M}})_1 - (\hat{\mathbf{X}}_{\mathfrak{M}})_{301} \right) \text{ in column 1,} \\ & \sqrt{n} \left((\hat{\mathbf{X}}_{\mathfrak{M}})_1 - (\hat{\mathbf{X}}_{\mathfrak{M}})_{601} \right) \text{ in column 2,} \\ & \sqrt{n} \left((\hat{\mathbf{X}}_{\mathfrak{M}})_{301} - (\hat{\mathbf{X}}_{\mathfrak{M}})_{601} \right) \text{ in column 3.} \end{aligned}$$

Each panel in the figure represents 100 Monte Carlo replicates (as the plotted points), and the limiting covariance structures are plotted as smooth curves. The different weightings in \mathfrak{M} are denoted via blue (always $\vec{w} = (1, 1, 1)$) and red. Figure 3 exhibits some interesting insights. First, the top left panel (denoted panel (1,1)) and the middle left panel (denoted panel (2,1)) capture the relationship between the omnibus matrix structure and the correlation as shown in Figure 2. Specifically, the weight of $A^{(3)}$ in block rows 1, 2 of \mathfrak{M} influences the scaling of the covariance matrix according to Eq. (15); we have $\rho(1, 2) = .8677$ in panel (1, 1) which provides more covariance shrinkage as compared to panel (2,1) where $\rho(1, 2) = .5950$ and as compared to panel (3,1) where the correlation is further dampened. Note that the third panel row correspond to the weighted matrix where its third block row does not satisfy *Assumption 2* from 4.1. In these cases, the estimated differences of the middle and right bottom panels do concentrate around 0, as the theory does not break down in this case.

Example 3. To demonstrate the types of correlation structures that can be created in the generalized omnibus embedding framework, we consider the following simple $m = 3$ example.

Consider

$$\boldsymbol{\alpha} = [\alpha(i, j)] = \begin{pmatrix} c & 3 - c & 0 \\ 3 - c & 2c - 3 & 3 - c \\ 0 & 3 - c & c \end{pmatrix} \quad (16)$$

for $c \in (2, 3]$. In this case, we can compute

$$\begin{aligned} \rho(1, 3) &= 1 - \left(\frac{c}{m}\right)^2 \\ \rho(1, 2) &= \rho(2, 3) = 1 - \frac{14c^2 - 54c + 54}{18} \end{aligned}$$

Plotting the two correlation values over a range of c in Figure 4, we see that even in this simple, one-parameter example we can achieve a structure in which embeddings corresponding to consecutive pairs of networks are significantly more correlated in the limit than the embeddings of $A^{(1)}$ and $A^{(3)}$.

5 Dampened correlation: Aplysia spike train analysis

We next consider applying our generalized omnibus methodology to a time series of networks derived from the Aplysia californica escape motor program of [20]. The motor program consists of a 20 min recording of the action potentials generated by 82 neurons in the dorsal pedal ganglion of an isolated brain preparation from the marine mollusk Aplysia californica. One minute into the recording a brief electrical stimulus was applied to pedal ganglion nerve 9 to elicit the animals rhythmic escape locomotion motor program. This consists of an initial rapid bursting lasting several cycles that drives the animals gallop behavior, followed by a slower rhythm persisting until the end of the recording that drives the animals crawling behavior. To extract a network time series from the recording, we binned the motor program into 24 bins, each approximately ≈ 50 second long; the binned motor program (with the second bin, containing the stimulus, highlighted) is pictured in Figure 5. Using the `meaRtools` package in R [17], we apply the STTC (spike time tiling correlation) method of [11] to convert each 50 second window into a weighted correlation matrix amongst the 82 neurons. Each of the 24 bins then yields one weighted graph on 82 vertices representing this correlation structure amongst the 82 neurons. The stimulus occurs then in the second of the 24 bins, followed by the gallop and crawling motor programs. The first bin is the unique bin corresponding to spontaneous firing activity.

5.1 Classical omnibus embeddings and correlation masking

Our motivation in the following analyses is to determine whether the classical or generalized OMNI methods can detect the distinct phases of behavior in the motor program. To this end, we first apply the classical omnibus embedding methodology on the Aplysia time series motor program. As in [26], we consider both M_n and to $\bar{M}_n := M_n - J_m \otimes \bar{A}$, where $\bar{A} = \frac{1}{m} \sum_{\ell} A^{(\ell)}$. The effect of centering by \bar{A} , while not fully theoretically explored, can be

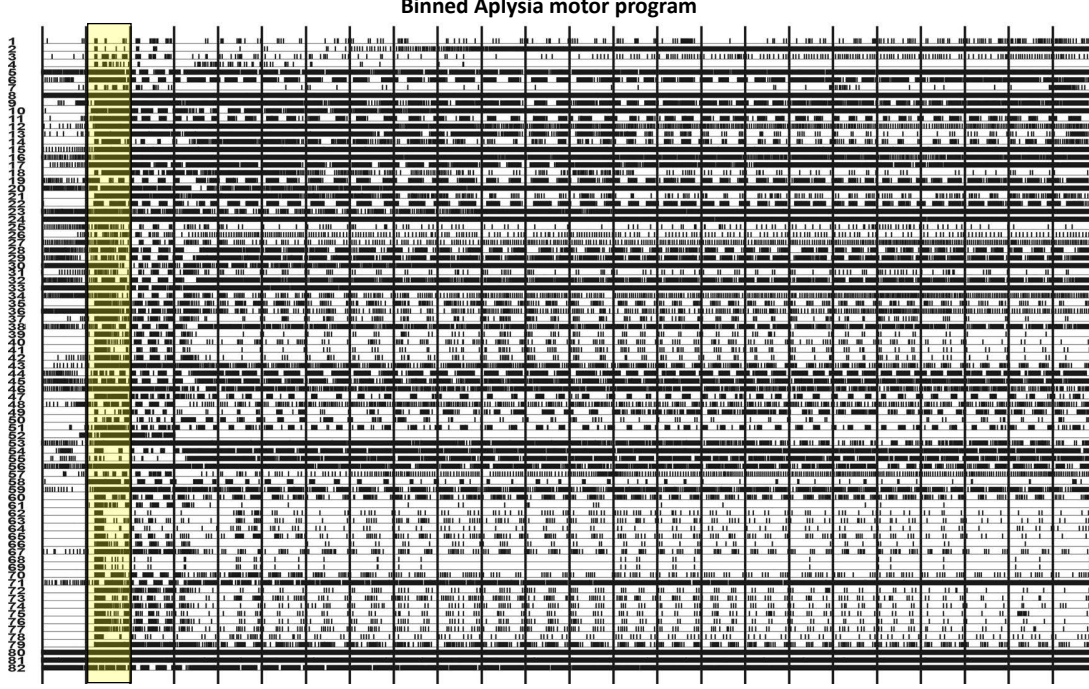


Figure 5: The 20 minute Aplysia escape motor program from [20], binned into 24 windows, each approximately 50 seconds in length. The stimulus happens one minute into the motor program, in the highlighted second bin.

understood as removing the common structure across the $A^{(\ell)}$ and effectively emphasizing the differences across the networks (whereas the uncentered omnibus embedding can be understood as emphasizing the similarities across the networks). In previous neuroscience applications of the omnibus methodology, centering has proven to be a key pre-processing tool for discovering biologically relevant trends in the data [26, 51].

In order to explore the impact of the flat correlation induced in the classical omnibus embedding, we embed the $\{(A^{(\ell)})_{\ell=1}^{24}\}$ into a common \mathbb{R}^d (where $d = 4$ in the uncentered and $d = 6$ in the centered cases, as chosen by locating the elbow in the scree plot as suggested by [61, 9]). Further isolating the impact of the stimulus and the evolution of the galloping and crawling phases of the motor program, we plot the average distance between the estimated latent positions for each vertex (as the bar heights) in the embedding between embedded graph 1 (res., embedded graph 2) and embedded graph k for each $k \in [m]$ (where the location of the bars in Figure 6 correspond to $k = 1, 2, \dots, 24$). To wit, we plot (where

$$\hat{\mathbf{X}}_{M_n} := [(\hat{\mathbf{X}}_{M_n}^{(1)})^T \mid (\hat{\mathbf{X}}_{M_n}^{(2)})^T \mid \dots \mid (\hat{\mathbf{X}}_{M_n}^{(m)})^T]^T,$$

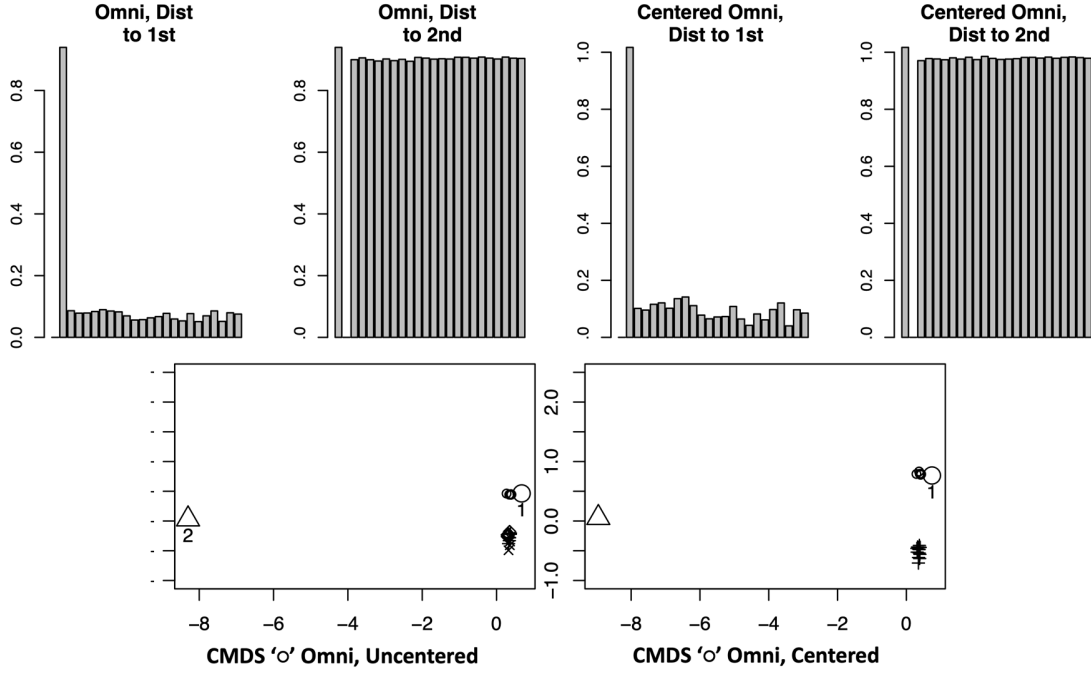


Figure 6: In the top row, we plot the average vertex distance (as the bar heights) in the embedding between graph 1 (res., graph 2) and graph k for each $k \in [m]$ in OMNI (where the bars are labeled $k = 1, 2, \dots, 24$). The left two panels correspond to uncentered OMNI, and the right two to centered OMNI. In the bottom panels (uncentered on the L, centered in the R), we compute the 24×24 distance matrices \mathbf{D} and $\bar{\mathbf{D}}$, and embed each into \mathbb{R}^2 . The resulting 24 data points are clustered using **Mclust** (clusters denoted by shape), and are plotted, with graphs 1 and 2 further labeled with their corresponding number.

and similarly for $\hat{\mathbf{X}}_{\bar{M}_n}$)

$$\begin{aligned} & \frac{1}{82} \sum_{i=1}^{82} \left\| \left(\hat{\mathbf{X}}_{M_n}^{(1)} \right)_i - \left(\hat{\mathbf{X}}_{M_n}^{(k)} \right)_i \right\|_2 \text{ in the top row, leftmost panel in Figure 6;} \\ & \frac{1}{82} \sum_{i=1}^{82} \left\| \left(\hat{\mathbf{X}}_{M_n}^{(2)} \right)_i - \left(\hat{\mathbf{X}}_{M_n}^{(k)} \right)_i \right\|_2 \text{ in the top row, second panel from the left in Figure 6;} \\ & \frac{1}{82} \sum_{i=1}^{82} \left\| \left(\hat{\mathbf{X}}_{\bar{M}_n}^{(1)} \right)_i - \left(\hat{\mathbf{X}}_{\bar{M}_n}^{(k)} \right)_i \right\|_2 \text{ in the top row, second panel from the right in Figure 6;} \\ & \frac{1}{82} \sum_{i=1}^{82} \left\| \left(\hat{\mathbf{X}}_{\bar{M}_n}^{(2)} \right)_i - \left(\hat{\mathbf{X}}_{\bar{M}_n}^{(k)} \right)_i \right\|_2 \text{ in the top row, rightmost panel in Figure 6.} \end{aligned}$$

From Figure 5, we see that if the omnibus embedding is able to detect the biologically distinct phases of this network time series, then the distance between the embeddings of graphs 1 and 2 will be large (as demonstrated in Figure 6), while the distance between graphs 2 and $k > 2$ will be increasing as the Aplysia transitions from galloping to crawling. Moreover, the

distance from graph 1 to graphs $k > 2$ should be large, as the Aplysia never returns to its spontaneous firing state in the motor program. While we see that the omnibus methodology demonstrates the capacity to detect the anomaly (namely, the stimulus) in the second graph, the flat correlation structure induced in the embedding space has the effect of masking the transition from galloping to crawling and creates an artificial similarity between graphs 1 and $k > 2$ in the embedded space.

Exploring this further, we compute the 24×24 distance matrices \mathbf{D} and $\bar{\mathbf{D}}$ ($\bar{\mathbf{D}}$ being defined analogously for $\hat{\mathbf{X}}_{\bar{M}_n}$), where

$$\mathbf{D} = [D_{i,j}] \text{ where } D_{i,j} = \|\hat{\mathbf{X}}_{M_n}^{(i)} - \hat{\mathbf{X}}_{M_n}^{(j)}\|_F. \quad (17)$$

These distance matrices are then each embedded into \mathbb{R}^2 (where $d = 2$ is, again, chosen by the elbow in the Scree plot as suggested by [61, 9]), and the 24 data points are clustered using **Mclust** [16]. The resulting clusters are plotted in the bottom row of Figure 6 (uncentered on the L, centered in the R). Points 1 and 2 (corresponding to graphs 1 and 2 resp.) are plotted with larger symbols and labeled. The cluster labels found by **Mclust** are as follows:

Graph	1	2	3	4	5	6	7	8	9	10	11	12
Uncentered	1	2	5	3	5	5	4	5	3	1	1	1
Centered	1	2	3	3	3	3	3	3	3	1	1	1

Graph	13	14	15	16	17	18	19	20	21	22	23	24
Uncentered	1	5	3	1	1	4	1	3	3	1	4	3
Centered	1	3	3	1	1	3	1	3	3	1	3	3

This reinforces that while the stimulus is detected (graph 2 is clustered apart from the others), the transition from stimulus to gallop and crawl and the distinct nature of graph 1 (as the only spontaneous firing state measurement) are masked in this analysis.

5.2 Dampened Omnibus Structure

In the above example, we see how the uniformity of the induced correlation in the classical omnibus embedding effectively masks much of the biologically relevant signal in the Aplysia motor program. In the Aplysia motor program, there is a dramatic spike in the data signal (the stimulus) followed by structured behavior and decay in spike intensity. In this case (and in many other time series settings where we are modeling the impact of anomalous events), it is natural to assume that the dependence between two networks at different times t_1, t_2 decays as their difference $|t_1 - t_2|$ gets bigger, and also decays over time as t_1, t_2 get bigger. This motivates the definition of the *dampened* omnibus matrix defined via

$$\mathfrak{M}_{damp}^{(i,j)} = \begin{cases} \frac{w_i A^{(i)} + A^{(j)}}{w_i + 1} & \text{if } i > j \\ A^{(i)} & \text{if } i = j \\ \frac{A^{(i)} + w_j A^{(j)}}{w_j + 1} & \text{if } i < j \end{cases}$$

where \vec{w} is a strictly increasing vector of weights. In the dampened omnibus matrix, \mathfrak{M}_{damp} , the relative contribution of each successive matrix (i.e., as $\ell > i$ increases in $A^{(\ell)}$) increases

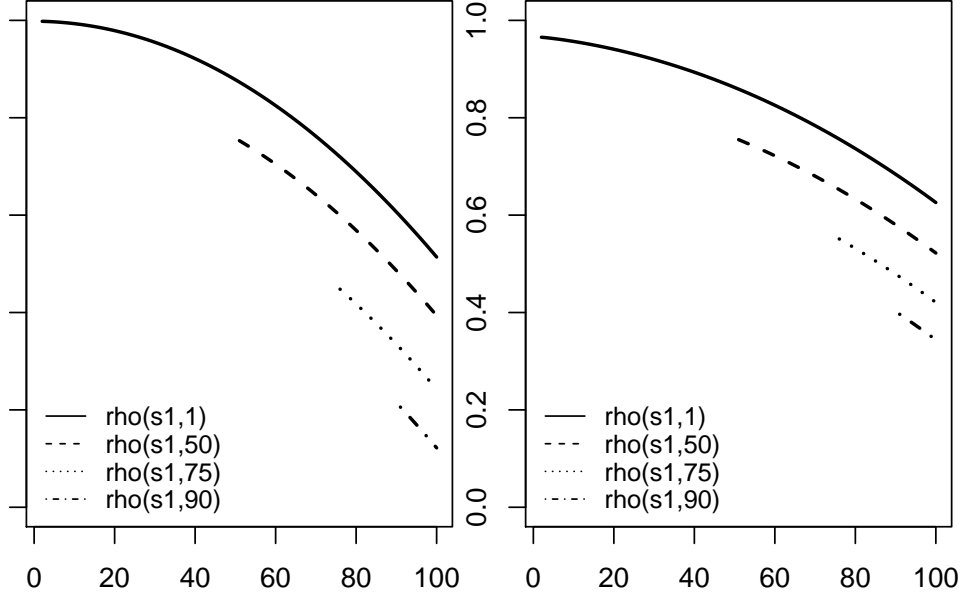


Figure 7: In the dampened omnibus embedding setting with $w_i = i$ (L) and $w_i = 1 + \log(i)$ (R) and $m = 100$, we plot $\rho(s_1, s_2)$ for $s_1 > s_2$, and $s_2 \in \{1, 50, 75, 100\}$.

in block-row i ; this (keeping the form of $\rho(s_1, s_2)$ in mind) can have the effect of decreasing the limiting induced correlation between $A^{(i)}$ and $A^{(\ell)}$ as $\ell > i$ increases. Analytically, the correlation structure can be computed as follows. Letting $h_1 = n(s_1 - 1) + i$ and $h_2 = n(s_2 - 1) + i$, where $s_1, s_2 \in [m]$, $s_1 > s_2$ and $i \in [n]$, we have that

$$\rho(s_1, s_2) = 1 - \frac{\eta(s_1, s_2)}{2m^2}$$

where

$$\begin{aligned} \eta(s_1, s_2) = & \frac{(s_2 - 1)(w_{s_1} - w_{s_2})^2}{(w_{s_1} + 1)^2(w_{s_2} + 1)^2} + \left(\frac{s_2 w_{s_2} + 1}{w_{s_2} + 1} + \sum_{t > s_2, t \neq s_1} \frac{1}{w_t + 1} \right)^2 \\ & + \sum_{s_2 < \ell < s_1} \left(\frac{w_\ell}{w_\ell + 1} - \frac{1}{w_{s_1} + 1} \right)^2 + \left(\frac{(s_1 - 1)w_{s_1} + 1}{w_{s_1} + 1} + \sum_{t > s_1} \frac{1}{w_t + 1} \right)^2 \end{aligned}$$

As an example, consider $w_i = i$ and $w_i = \log(i) + 1$, and $m = 100$. In Table 1 below, we list the limiting induced correlation for a number of (s_1, s_2) pairs, offering a sharp contrast to the flat induced correlation in the classical omnibus setting. In Figure 7, in the $m = 100$ case, we further plot $\rho(s_1, s_2)$ for $s_1 > s_2$, and $s_2 \in \{1, 50, 75, 100\}$. We see the general trend that $\rho(s_1, s_2)$ is decreasing as s_1 increases for a fixed s_2 (and as $\rho(\cdot, \cdot)$ is a symmetric function, as s_2 increases for a fixed s_1). Note the level of correlation decays differs dramatically across the two figures, as the slower growth of the weights in the $w_i = 1 + \log(i)$ setting allows for a slower decay in the pairwise correlations. We are presently working to generalize this idea (i.e., choosing the right growth rate in \vec{w} to induce the right amount of decaying correlation).

$m = 100$	dampened $w_i = i$	dampened $w_i = 1 + \log(i)$	classical
$s_1 = 1, s_2 = 2$.9981	.9653	.75
$s_1 = 1, s_2 = 50$.8781	.8622	.75
$s_1 = 1, s_2 = 100$.5140	.6259	.75
$s_1 = 49, s_2 = 50$.7626	.7618	.75
$s_1 = 50, s_2 = 100$.3936	.5222	.75
$s_1 = 99, s_2 = 100$.0391	.2918	.75

Table 1: In the $m = 100$ and $m = 10$ settings, we list the limiting induced correlation for dampened omnibus and classical omnibus for a number of (s_1, s_2) pairs

In both cases, the decaying correlation structure appears well-suited for the Aplysia motor program, as it precisely allows for a large correlation at early time-points (corresponding to the dampening of signal after an anomalous event) that dissipates in time. We will explore this further in the next section.

5.3 Dampened spike train analysis

Since the generalized omnibus embedding permits additional degrees of freedom for the off-diagonal entries, a richer spectrum of induced correlation is possible. The dampened omnibus embedding, in particular, is designed to weaken cross-graph interplay over time. Given that the correlation homogeneity of the classical omnibus makes inter-network changes less apparent, it is natural to ask if an appropriately-calibrated dampened omnibus embedding can detect what the more limited classical omnibus can not.

We next apply the methodology of Section 5.1 with $w_i = i$ (results with $w_i = \log(i) + 1$ being similar), using both \mathfrak{M}_{damp} (uncentered) and $\bar{\mathfrak{M}}_{damp} := \mathfrak{M}_{damp} - J_m \otimes \bar{A}$ (centered). Results are summarized in Figure 8 where \mathbf{D}_d and $\bar{\mathbf{D}}_d$ are the corresponding distance matrices from Eq. 17 in the dampened and centered, dampened settings respectively. We again see that, both in the centered and uncentered settings, dampened omnibus is able to isolate the stimulus in the second graph. However, unlike in the standard omnibus setting, dampened omnibus is able to tease out additional relevant structure including the uniqueness of graph 1, the transition from gallop to crawl and an unstable dynamic in the crawling motor program. In this dampened setting with weights $w_i = i$ (results with $w_i = \log(i) + 1$ being similar), the cluster labels found by `Mclust` are as follows:

Graph	1	2	3	4	5	6	7	8	9	10	11	12
Uncentered	1	2	3	3	3	3	3	3	3	4	4	4
Centered	1	2	3	3	3	3	4	3	3	5	9	5

Graph	13	14	15	16	17	18	19	20	21	22	23	24
Uncentered	4	5	5	4	4	5	4	5	5	4	5	5
Centered	5	6	4	9	7	8	7	6	10	11	12	12

In both the centered and uncentered cases, we further see that the clustering is better able to isolate graph 1 (the spontaneous firing state graph) than in the classical omnibus setting.

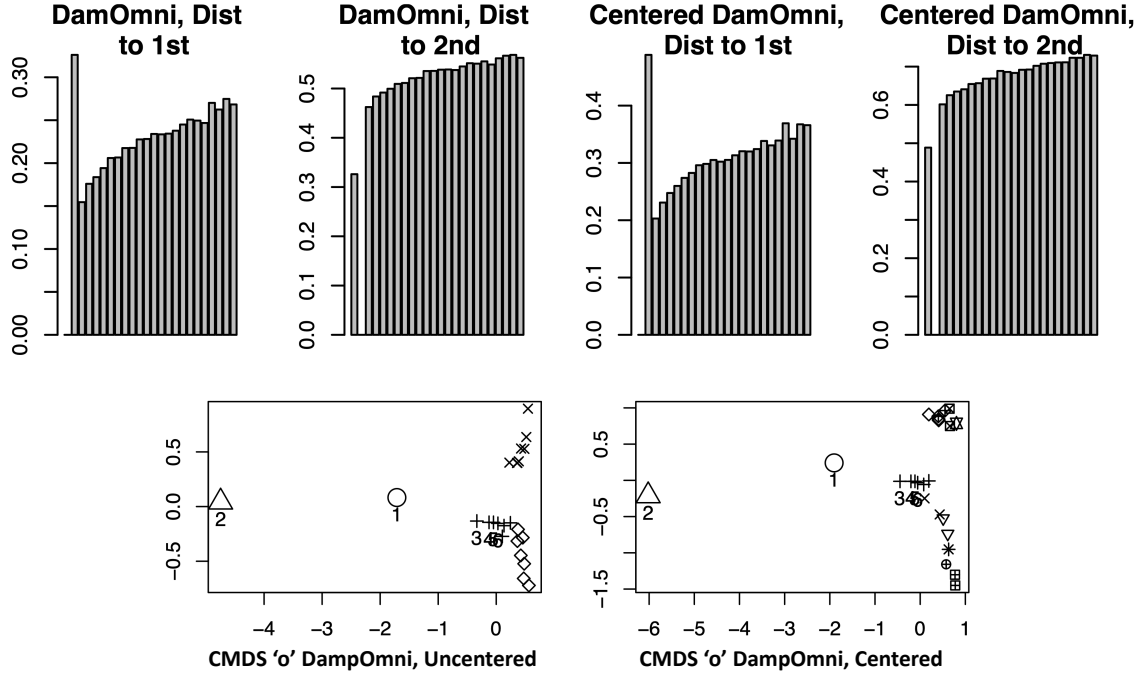


Figure 8: Using weights $w_i = i$ in dampened OMNI: In the top row, we plot the average vertex distance (as the bar heights) in the embedding between graph 1 (res., graph 2) and graph k for each $k \in [m]$ in dampened OMNI (where the bars are labeled $k = 1, 2, \dots, 24$). The left two panels correspond to uncentered dampened OMNI, and the right two to centered dampened OMNI. In the bottom panels (uncentered on the L, centered in the R), we compute the 24×24 distance matrices \mathbf{D}_d and $\bar{\mathbf{D}}_d$, and embed each into an appropriately chosen \mathbb{R}^d ($d = 2$ in the uncentered, and $d = 3$ in the centered cases, plotting here the first two dimensions of the embedding). The resulting 24 data points are clustered using `Mclust` (clusters denoted by shape), and are plotted, with graphs 1–6 further labeled with their corresponding number.

Moreover, the clustering of graphs 3–9 and the CMDS graph embedding, shows that the dampened setting is better able to capture (imperfectly) the transition from galloping in bins 3 and 4 to crawling in bins 5–24. In the uncentered case, clustering yields classes that progress in orderly fashion over the first half of the motor program, after which states irregularly alternate between 4 and 5, suggesting an unstable dynamic to the program not apparent from simple visual inspection of the firing traces. In the centered setting, while an unstable dynamic is present (from a visual inspection of the CMDS projection), the alternating is less regular and there is more differentiation within the alternating classes.

Here, the dampened omnibus structure allows us to better tease out the biologically relevant structure in the data; namely, the distinct nature of graph 1, the transition from gallop to crawl, the unstable dynamic in the crawling. Indeed, from Figure 6, we see that the flat correlation structure induced by classical OMNI (with or without centering) masks much of this latent structure in these biological networks, while the dampened structure induces the right correlation and (with and without centering) both uncovers and clarifies

this neuroscientifically relevant signal in the data.

6 Conclusion

One of the key features of the omnibus embedding methodology is its theoretical tractability, because the method is particularly amenable to the rigorous analysis of its component pieces. One such component is the level of induced correlation introduced across networks in the omnibus framework, and in this paper we provide a first step toward understanding this correlation in the classical setting and altering the classical setting to produce more exotic correlation structures. The implications of this are many, both in the analysis of real data (Section 5), and in the setting where we desire the omnibus method to transform i.i.d. data into embedded data with latent correlation structure. While this paper offers a first step towards answering these questions, there is much yet to do.

A natural question is whether, given a feasible correlation structure for a collection of networks, we can choose weights in the generalized omnibus setting that would (from i.i.d. networks) reproduce this structure in the embedded space. Representing the correlation matrix via $\boldsymbol{\rho} = [\rho(s_1, s_2)] \in \mathbb{R}^{m \times m}$ and the matrix of weights $\boldsymbol{\alpha} = [\alpha(s_1, s_2)] \in \mathbb{R}^{m \times m}$, we see that this amounts to finding $\boldsymbol{\alpha}$ solving

$$\boldsymbol{\rho} = \mathbf{1} - \frac{1}{2m^2} \mathbf{D}_{\boldsymbol{\alpha}}, \quad (18)$$

where

$$\mathbf{D}_{\boldsymbol{\alpha}} = [\mathbf{D}_{\boldsymbol{\alpha}}(i, j)] = [\|\alpha(i, \cdot) - \alpha(j, \cdot)\|_2^2].$$

This would be easily solved (if a solution exists) using the tools of multidimensional scaling [7] if not for the condition that each $\alpha(i, \cdot)$ must be nonnegative and sum to m . We are exploring possible approximation approaches for this problem, including alternately projecting onto the cone of distance matrices [58] and the polytope defining the constraints on the α 's. An approximate solution for this is essential, as it would allow us to use the generalized omnibus framework to induce a given correlation structure in embedded space.

In the absence of a general solution, there are a number of \mathfrak{M} we could consider that would induce differing limiting levels of correlation amongst the network pairs. For example, we could consider the forward omnibus matrix \mathfrak{M}_{for} , where

$$\mathfrak{M}_{for}^{(i,j)} = \begin{cases} \frac{(i-1)A^{(j)} + A^{(i)}}{i} & \text{if } i > j \\ A^{(i)} & \text{if } i = j \\ \frac{(j-1)A^{(i)} + A^{(j)}}{j} & \text{if } i < j \end{cases}$$

Comparing this to the dampened setting in the $m = 100$ case, we have the following analogue of Table 1 in which we show the limiting induced correlation between $A^{(i)}$ and $A^{(j)}$ for a variety of (i, j) pairs (where in the dampened case, we are considering $w_i = i$),

$m = 100$	dampened	forward
$s_1 = 1, s_2 = 2$.9981	.0914
$s_1 = 1, s_2 = 50$.8781	.4136
$s_1 = 1, s_2 = 100$.5140	.5443
$s_1 = 49, s_2 = 50$.7626	.7301
$s_1 = 50, s_2 = 100$.3936	.8663
$s_1 = 99, s_2 = 100$.0391	.9964

We see that \mathfrak{M}_{for} can be used to model time series where the correlation is progressively building up as the series progresses. While the understanding of the limiting induced correlation structure given in Eq. 14 does allow for these example-based constructions, a more automated approach is needed for broader applications.

We lastly touch on the structure of the omnibus mean matrix $\tilde{P} = J_m \otimes P$. This structure maintains the low-rankedness of P in \tilde{P} and allows for the leading d eigenvectors of P to be related to those of \tilde{P} (indeed $\tilde{\mathbf{I}} \otimes U_P$ provides a basis for the leading d -dimensional eigenspace of \tilde{P}). If we consider other structures in the Kronecker product that have the form $E \otimes P$, with the restriction that $\tilde{\mathbf{I}}$ is a leading eigenvector of E , can we replicate the omnibus analysis? We are exploring this at present with examples of interest including E having ring-graph structure. While more complex E will necessarily violate the low-rankedness of \tilde{P} , we are exploring if there is still sufficient concentration (about $\tilde{\mathbf{I}} \otimes \mathbf{X}$) of the leading d -dimensional eigenspace of \mathfrak{M} in order to still make use of a low-rank approximation of \tilde{P} .

Acknowledgements This material is based on research sponsored by the Air Force Research Laboratory and DARPA under agreement number FA8750-20-2-1001. The U.S. Government is authorized to reproduce and distribute reprints for Governmental purposes notwithstanding any copyright notation thereon. The views and conclusions contained herein are those of the authors and should not be interpreted as necessarily representing the official policies or endorsements, either expressed or implied, of the Air Force Research Laboratory and DARPA or the U.S. Government. The authors also gratefully acknowledge the support of NIH grant BRAIN U01-NS108637. We also gratefully acknowledge illustrative conversations with Profs. Minh Tang, Keith Levin, Daniel Sussman and Carey Priebe that helped shaped this work.

References

- [1] J. Arroyo, A. Athreya, J. Cape, G. Chen, C. E. Priebe, and J. T. Vogelstein. Inference for multiple heterogeneous networks with a common invariant subspace. *Journal of Machine Learning Research*, accepted for publication, 2020.
- [2] D. Asta and C. Shalizi. Geometric network comparison. Arxiv preprint at <http://arxiv.org/abs/1411.1350>, 2014.
- [3] A. Athreya, D. E. Fishkind, K. Levin, , V. Lyzinski, Y. Park, Y. Qin, D. L. Sussman, M. Tang, J. T. Vogelstein, and C. E. Priebe. Statistical inference on random dot product graphs: a survey. *Journal of Machine Learning Research*, 18, 2018.

- [4] A. Athreya, V. Lyzinski, D. J. Marchette, C. E. Priebe, D. L. Sussman, and M. Tang. A limit theorem for scaled eigenvectors of random dot product graphs. *Sankhya A*, 78:1–18, 2016.
- [5] A. Athreya, M. Tang, Y. Park, and C. E. Priebe. On estimation and inference in latent structure random graphs. To appear in *Statistical Science*; Arxiv preprint at <http://arxiv.org/abs/1806.01401>, 2018.
- [6] R. Bhatia. *Matrix Analysis*. Springer, 1997.
- [7] I. Borg and P. J. F. Groenen. *Modern multidimensional scaling: Theory and applications*. Springer Science & Business Media, 2005.
- [8] J. Cape, M. Tang, and C. E. Priebe. The two-to-infinity norm and singular subspace geometry with applications to high-dimensional statistics. *Annals of Statistics*, 2018. Arxiv preprint at <http://arxiv.org/abs/1705.10735>.
- [9] S. Chatterjee. Matrix estimation by universal singular value thresholding. *Annals of Statistics*, 43:177–214, 2015.
- [10] K. L. Chung. *A course in probability theory*. Academic Press, 3 edition, 2001.
- [11] C. S. Cutts and S. J. Eglén. Detecting pairwise correlations in spike trains: an objective comparison of methods and application to the study of retinal waves. *Journal of Neuroscience*, 34(43):14288–14303, 2014.
- [12] C. Davis and W. Kahan. The rotation of eigenvectors by a perturbation. III. *SIAM Journal on Numerical Analysis*, 7:1–46, 1970.
- [13] B. Draves and D. L. Sussman. Bias-variance tradeoffs in joint spectral embeddings. *arXiv preprint arXiv:2005.02511*, 2020.
- [14] D. Durante and D. B. Dunson. Bayesian inference on group differences in brain networks. *Bayesian Analysis*, 13(1), 2018.
- [15] D. Durante, D. B. Dunson, and J. T. Vogelstein. Nonparametric bayes modeling of populations of networks. *Journal of the American Statistical Association*, 112(520):1516–1530, 2017.
- [16] C. Fraley and A. E. Raftery. Model-based clustering, discriminant analysis and density estimation. *Journal of the American Statistical Association*, 97:611–631, 2002.
- [17] S. Gelfman, Q. Wang, Y. Lu, D. Hall, C. D. Bostick, R. Dhindsa, M. Halvorsen, K. M. McSweeney, E. Cotterill, and T. Edinburgh. meartools: An r package for the analysis of neuronal networks recorded on microelectrode arrays. *PLoS computational biology*, 14(10):e1006506, 2018.
- [18] J. C. Gower. Generalized procrustes analysis. *Psychometrika*, 40:33–51, 1975.

- [19] A. Grover and J. Leskovec. node2vec: Scalable feature learning for networks. In *Proceedings of the 22nd ACM SIGKDD international conference on Knowledge discovery and data mining*, pages 855–864, 2016.
- [20] E. S. Hill, J. W. Brown, and W. N. Frost. Photodiode-based optical imaging for recording network dynamics with single-neuron resolution in non-transgenic invertebrates. *J. Vis. Exp.*, 161, e61623, 2020.
- [21] P. D. Hoff, A. E. Raftery, and M. S. Handcock. Latent space approaches to social network analysis. *Journal of the American Statistical Association*, 97(460):1090–1098, 2002.
- [22] P. D. Hoff, A. E. Raftery, and M. S. Handcock. Latent space approaches to social network analysis. *Journal of the American Statistical Association*, 97:1090–1098, 2002.
- [23] P. W. Holland, K. Laskey, and S. Leinhardt. Stochastic blockmodels: First steps. *Social Networks*, 5:109–137, 1983.
- [24] R. Horn and C. Johnson. *Matrix Analysis*. Cambridge University Press, 1985.
- [25] M. Kivelä, A. Arenas, M. Barthélemy, J. P. Gleeson, Y. Moreno, and M. A. Porter. Multilayer networks. *Journal of complex networks*, 2(3):203–271, 2014.
- [26] K. Levin, A. Athreya, M. Tang, V. Lyzinski, and C. E. Priebe. A central limit theorem for an omnibus embedding of random dot product graphs. *arXiv preprint arXiv:1705.09355*, 2017.
- [27] Y. Li and H. Li. Two-sample test of community memberships of weighted stochastic block models. *arXiv preprint arXiv:1811.12593*, 2018.
- [28] L. Lu and X. Peng. Spectra of edge-independent random graphs. *Electronic Journal of Combinatorics*, 20, 2013.
- [29] V. Lyzinski. Information recovery in shuffled graphs via graph matching. Arxiv preprint at <http://arxiv.org/abs/1605.02315>, 2016.
- [30] V. Lyzinski and D. L. Sussman. Matchability of heterogeneous networks pairs. *Information and Inference: A Journal of the IMA*, 01 2020. iaz031.
- [31] V. Lyzinski, D. L. Sussman, D. E. Fishkind, H. Pao, L. Chen, J. T. Vogelstein, Y. Park, and C. E. Priebe. Spectral clustering for divide-and-conquer graph matching. *Parallel Computing*, 47:70–87, 2015.
- [32] V. Lyzinski, D. L. Sussman, M. Tang, A. Athreya, and C. E. Priebe. Perfect clustering for stochastic blockmodel graphs via adjacency spectral embedding. *Electronic Journal of Statistics*, 8:2905–2922, 2014.
- [33] V. Lyzinski, M. Tang, A. Athreya, Y. Park, and C. E. Priebe. Community detection and classification in hierarchical stochastic blockmodels. *IEEE Transactions in Network Science and Engineering*, 4:13–26, 2017.

- [34] A. Myronenko and X. Song. Point set registration: Coherent point drift. *IEEE transactions on pattern analysis and machine intelligence*, 32(12):2262–2275, 2010.
- [35] A. M. Nielsen and D. Witten. The multiple random dot product graph model. *arXiv preprint arXiv:1811.12172*, 2018.
- [36] R. I. Oliveira. Concentration of the adjacency matrix and of the Laplacian in random graphs with independent edges. <http://arxiv.org/abs/0911.0600>, 2009.
- [37] H. G. Patsolic, Y. Park, V. Lyzinski, and C. E. Priebe. Vertex nomination via seeded graph matching. *Statistical Analysis and Data Mining: The ASA Data Science Journal*, 13(3):229–244, 2020.
- [38] S. Paul and Y. Chen. Consistent community detection in multi-relational data through restricted multi-layer stochastic blockmodel. *Electronic Journal of Statistics*, 10(2):3807–3870, 2016.
- [39] S. Paul and Y. Chen. Spectral and matrix factorization methods for consistent community detection in multi-layer networks. *The Annals of Statistics*, 48(1):230–250, 2020.
- [40] C. E. Priebe, Y. Park, J. T. Vogelstein, J. M. Conroy, V. Lyzinski, M. Tang, A. Athreya, J. Cape, and E. Bridgeford. On a two-truths phenomenon in spectral graph clustering. *Proceedings of the National Academy of Sciences*, 116(13):5995–6000, 2019.
- [41] L. F.R. Ribeiro, P. H.P. Saverese, and D. R. Figueiredo. struc2vec: Learning node representations from structural identity. In *Proceedings of the 23rd ACM SIGKDD international conference on knowledge discovery and data mining*, pages 385–394, 2017.
- [42] K. Rohe, S. Chatterjee, and B. Yu. Spectral clustering and the high-dimensional stochastic blockmodel. *Annals of Statistics*, 39:1878–1915, 2011.
- [43] P. Rubin-Delanchy, C. E. Priebe, and M. Tang. The generalised random dot product graph. Arxiv preprint available at <http://arxiv.org/abs/1709.05506>, 2017.
- [44] D. L. Sussman, M. Tang, D. E. Fishkind, and C. E. Priebe. A consistent adjacency spectral embedding for stochastic blockmodel graphs. *Journal of the American Statistical Association*, 107:1119–1128, 2012.
- [45] M. Tang, A. Athreya, D. L. Sussman, V. Lyzinski, Y. Park, and C. E. Priebe. A semiparametric two-sample hypothesis testing problem for random dot product graphs. *Journal of Computational and Graphical Statistics*, 26:344–354, 2017.
- [46] M. Tang, A. Athreya, D. L. Sussman, V. Lyzinski, and C. E. Priebe. A nonparametric two-sample hypothesis testing problem for random dot product graphs. *Bernoulli*, 23:1599–1630, 2017.
- [47] M. Tang, J. Cape, and C. E. Priebe. Asymptotically efficient estimators for stochastic blockmodels: The naive mle, the rank-constrained mle, and the spectral. *arXiv preprint arXiv:1710.10936*, 2017.

- [48] M. Tang and C. E. Priebe. Limit theorems for eigenvectors of the normalized laplacian for random graphs. *Annals of Statistics*, 2018. In press.
- [49] R. Tang, M. Ketcha, A. Badea, E. D. Calabrese, D. S. Margulies, J. T. Vogelstein, C. E. Priebe, and D. L. Sussman. Connectome smoothing via low-rank approximations. *IEEE transactions on medical imaging*, 38(6):1446–1456, 2018.
- [50] R. Vershynin. *High-dimensional probability: An introduction with applications in data science*, volume 47. Cambridge university press, 2018.
- [51] N. Wang, R. J. Anderson, D. G. Ashbrook, V. Gopalakrishnan, Y. Park, C. E. Priebe, Y. Q., J. T. Vogelstein, R. W. Williams, and G. A. Johnson. Node-specific heritability in the mouse connectome. *bioRxiv*, page 701755, 2019.
- [52] S. Wang, J. Arroyo, J. T. Vogelstein, and C. E. Priebe. Joint embedding of graphs. *IEEE Transactions on Pattern Analysis and Machine Intelligence*, 2019.
- [53] F. Xie and Y. Xu. Efficient estimation for random dot product graphs via a one-step procedure. *arXiv preprint arXiv:1910.04333*, 2019.
- [54] S. Young and E. Scheinerman. Random dot product graph models for social networks. In *Proceedings of the 5th international conference on algorithms and models for the web-graph*, pages 138–149, 2007.
- [55] Y. Yu, T. Wang, and R. J. Samworth. A useful variant of the Davis-Kahan theorem for statisticians. *Biometrika*, 102:315–323, 2015.
- [56] A. Zhang. Cross: Efficient low-rank tensor completion. *The Annals of Statistics*, 47(2):936–964, 2019.
- [57] A. Zhang and D. Xia. Tensor svd: Statistical and computational limits. *IEEE Transactions on Information Theory*, 64(11):7311–7338, 2018.
- [58] L. Zhang, G. Wahba, and M. Yuan. Distance shrinkage and euclidean embedding via regularized kernel estimation. *arXiv preprint arXiv:1409.5009*, 2014.
- [59] Y. Zhang. Consistent polynomial-time unseeded graph matching for lipschitz graphons. *arXiv preprint arXiv:1807.11027*, 2018.
- [60] Y. Zhang. Unseeded low-rank graph matching by transform-based unsupervised point registration. *arXiv preprint arXiv:1807.04680*, 2018.
- [61] M. Zhu and A. Ghodsi. Automatic dimensionality selection from the scree plot via the use of profile likelihood. *Computational Statistics and Data Analysis*, 51:918–930, 2006.

A Proofs of main results

Herein we collect the proofs of the main theoretical results of the paper. Before proving the theorems, we will first establish some convenient asymptotic notation for our theory moving forward.

Definition A.1. *Given a sequence of events $\{E_n\} \in \mathcal{F}$, where $n = 1, 2, \dots$, we say that E_n occurs*

- i. asymptotically almost surely and write E_n a.a.s. if $\mathbb{P}(E_n) \rightarrow 1$ as $n \rightarrow \infty$.*
- ii. with high probability, and write E_n w.h.p. , if for some $a_0 \geq 2$, there exists finite positive constant A_0 depending only on a_0 such that*

$$\mathbb{P}[E_n^c] \leq A_0 n^{-a_0}$$

for all n .

We note that E_n occurring w.h.p. is stronger than E_n occurring a.a.s., as w.h.p. implies, by the Borel-Cantelli Lemma [10], that $\mathbb{P}(\limsup E_n) = 1$ and with probability 1 all but finitely many E_n occur.

The following Lemma will be needed in the proof of Theorem 3 at Section A.2. For a proof, see [8].

Lemma 1. *For $A \in \mathbb{R}^{p_1 \times p_2}$ and $B \in \mathbb{R}^{p_2 \times p_3}$, we have the following:*

$$\begin{aligned} \|A\|_{2 \rightarrow \infty} &= \max_{i \in [p_1]} \|A_i\|_2; \\ \|AB\|_{2 \rightarrow \infty} &\leq \|A\|_{2 \rightarrow \infty} \|B\|_2; \end{aligned}$$

where A_i denotes the i -th row of A .

A.1 Proof of Theorem 1

For each $n \geq 1$, we write the spectral decomposition of the positive semidefinite P_n via

$$P_n = \mathbf{X}_n \mathbf{X}_n^T = U_{P_n} S_{P_n} U_{P_n}^T.$$

In the sequel, we will suppress the implicit dependence on n . Let the singular value decomposition of $U_P^T U_{B(1)}$ be denoted $W_{11} D_1 W_{12}^T$ and define $W^{*,1} = W_{11} W_{12}^T$. Similarly, let the singular value decomposition of $U_P^T U_{B(2)}$ be denoted $W_{21} D_2 W_{22}^T$ and define $W^{*,2} = W_{21} W_{22}^T$. As in the proof of Theorem 9 in [3], we have that for each $k = 1, 2$ and fixed index i ,

$$\sqrt{n} \left(U_{B^{(k)}} S_{B^{(k)}}^{1/2} - U_P S_P^{1/2} W^{*,k} \right)_i = \sqrt{n} \left((B^{(k)} - P) U_P S_P^{-1/2} W^{*,k} \right)_i + O(n^{-1/2} \log n) \quad (19)$$

with high probability. Letting W_n be a sequence of orthogonal matrices such that

$$U_{P_n} S_{P_n}^{1/2} W_n = \mathbf{X}_n$$

for all $n \geq 1$, we have then that, again with high probability,

$$\sqrt{n} \left(U_{B^{(k)}} S_{B^{(k)}}^{1/2} (W^{*,k})^T W - U_P S_P^{1/2} W \right)_i = \sqrt{n} \left((B^{(k)} - P) U_P S_P^{-1/2} W \right)_i + O(n^{-1/2} \log n) \quad (20)$$

It follows then that for fixed i , we have with high probability

$$\begin{aligned} & \sqrt{n} \left(U_{B^{(1)}} S_{B^{(1)}}^{1/2} (W^{*,1})^T W - U_{B^{(2)}} S_{B^{(2)}}^{1/2} (W^{*,2})^T W \right)_i \\ &= \sqrt{n} \left(U_{B^{(1)}} S_{B^{(1)}}^{1/2} (W^{*,1})^T W - U_P S_P^{1/2} W \right)_i + \sqrt{n} \left(U_P S_P^{1/2} W - U_{B^{(2)}} S_{B^{(2)}}^{1/2} (W^{*,2})^T W \right)_i \\ &= \sqrt{n} \left((B^{(1)} - P) U_P S_P^{-1/2} W \right)_i - \sqrt{n} \left((B^{(2)} - P) U_P S_P^{-1/2} W \right)_i + O\left(\frac{\log n}{\sqrt{n}}\right) \\ &= \sqrt{n} \left((B^{(1)} - B^{(2)}) U_P S_P^{-1/2} W \right)_i + O\left(\frac{\log n}{\sqrt{n}}\right). \end{aligned} \quad (21)$$

Next note that

$$\begin{aligned} \sqrt{n} \left((B^{(1)} - B^{(2)}) U_P S_P^{-1/2} W \right)_i &= \sqrt{n} \left((B^{(1)} - B^{(2)}) \mathbf{X} \right)_i W^T S_P^{-1} W \\ &= \sqrt{n} \left(\sum_j (B_{i,j}^{(1)} - B_{i,j}^{(2)}) X_j \right) W^T S_P^{-1} W \\ &= \left(n^{-1/2} \sum_j (B_{i,j}^{(1)} - B_{i,j}^{(2)}) X_j \right) (n W^T S_P^{-1} W) \end{aligned}$$

Conditioning on $X_i = x_i$, the sum

$$n^{-1/2} \sum_j (B_{i,j}^{(1)} - B_{i,j}^{(2)}) X_j$$

is a scaled sum of $n - 1$ i.i.d random variables (the $(B_{i,j}^{(1)} - B_{i,j}^{(2)}) X_j$), each with mean

$$\begin{aligned} \mathbb{E}((B_{i,j}^{(1)} - B_{i,j}^{(2)}) X_j) &= \mathbb{E}(\mathbb{E}((B_{i,j}^{(1)} - B_{i,j}^{(2)}) X_j | X_j)) \\ &= \mathbb{E}(X_j \mathbb{E}(B_{i,j}^{(1)} - B_{i,j}^{(2)} | X_j)) = 0 \end{aligned}$$

and covariance matrix

$$\tilde{\Sigma}(x_i) = 2(1 - \rho) \mathbb{E}[X_j X_j^T (x_i^T X_j - (x_i^T X_j)^2)],$$

as

$$\begin{aligned} \text{Cov}((B_{i,j}^{(1)} - B_{i,j}^{(2)}) X_j) &= \mathbb{E}[(B_{i,j}^{(1)} - B_{i,j}^{(2)})^2 X_j X_j^T] \\ &= \mathbb{E}(\mathbb{E}[(B_{i,j}^{(1)} - B_{i,j}^{(2)})^2 X_j X_j^T | X_j]) \\ &= \mathbb{E}(X_j X_j^T \mathbb{E}[(B_{i,j}^{(1)} - B_{i,j}^{(2)})^2 | X_j]) \\ &= \mathbb{E}(X_j X_j^T \mathbb{E}[(B_{i,j}^{(1)})^2 + (B_{i,j}^{(2)})^2 - 2B_{i,j}^{(1)} B_{i,j}^{(2)} | X_j]) \\ &= \mathbb{E}(X_j X_j^T [2x_i^T X_j - 2x_i^T X_j (x_i^T X_j + \rho(1 - x_i^T X_j))]) \\ &= \mathbb{E}(X_j X_j^T [2x_i^T X_j - 2(x_i^T X_j)^2 - \rho 2(1 - x_i^T X_j) x_i^T X_j]) \\ &= 2(1 - \rho) \mathbb{E}[X_j X_j^T (x_i^T X_j - (x_i^T X_j)^2)]. \end{aligned}$$

The classical multivariate central limit theorem then yields

$$n^{-1/2} \sum_j (B_{i,j}^{(1)} - B_{i,j}^{(2)}) X_j \xrightarrow{D} \mathcal{N}(0, 2(1 - \rho) \mathbb{E}[X_j X_j^T (x_i^T X_j - (x_i^T X_j)^2)]). \quad (22)$$

The strong law of large numbers (SLLN) ensures that $\frac{1}{n} \mathbf{X}^T \mathbf{X} = \frac{1}{n} W^T S_P W \xrightarrow{a.s.} \Delta$ and therefore, $n W^T S_P^{-1} W \xrightarrow{a.s.} \Delta^{-1}$. Therefore, by the multivariate Slutsky's Theorem, conditional on $X_i = x_i$, we have that

$$\sqrt{n} \left((B^{(1)} - B^{(2)}) U_P S_P^{-1/2} W \right)_i \xrightarrow{D} \mathcal{N}(0, \tilde{\Sigma}(x_i, \rho)). \quad (23)$$

The result then follows from multivariate Slutsky's applied to Eq. (21) and (23), and integrating the above display over the possible values of x_i with respect to distribution F .

A.2 Proof of Theorem 3

To ease notation, in this proof we will suppress the explicit dependence on n in the subscript of $\mathfrak{M} = \mathfrak{M}_n$, $\tilde{P} = \tilde{P}_n$, noting that this dependence is to be implicitly understood throughout. Recall that the spectral decomposition of \tilde{P} is given by

$$\tilde{P} = \mathbb{E}(\mathfrak{M}) = U_{\tilde{P}} S_{\tilde{P}} U_{\tilde{P}}^T,$$

where $U_{\tilde{P}} \in \mathbb{R}^{mn \times d}$ and $S_{\tilde{P}} \in \mathbb{R}^{d \times d}$. Also recall that the adjacency spectral embedding of \mathfrak{M} is given by $\text{ASE}(\mathfrak{M}, d) = U_{\mathfrak{M}} S_{\mathfrak{M}}^{1/2}$.

To prove Theorem 3, we adapt the proof of Theorem 1 in [26]. The main difficulty in this adaptation is the more complex structure of the general \mathfrak{M} , which requires a number of modifications in the proof reasoning:

- The proofs of the Bernstein matrix concentration result and Lemma 4 necessitate a more delicate decomposition of \mathfrak{M} in order to leverage classical concentration inequality results. Moreover, the constructed proof of Lemma 5 highlights how the coefficients matrices $C^{(l)}$ of the adjacency matrices $A^{(l)}$ in \mathfrak{M} fully characterize the omnibus matrix \mathfrak{M} .
- We adapt the general exchangeability result in the proof of Lemma 5 of [26] (used there to bound the term ' B_1 ') to our current setting, and the general block-form of \mathfrak{M} still allows for a weaker (within block) exchangeability argument to be employed, which is sufficient for our purposes.
- The weights in the \mathfrak{M} matrix necessitate novel decompositions to compute the relevant covariance structures.
- Considering row-wise differences of \mathfrak{M} is a key contribution to the literature.

The overall layout of the proof is as follows. Let $\hat{\mathbf{X}}_{\mathfrak{M}_n} = \text{ASE}(\mathfrak{M}_n, d) = U_{\mathfrak{M}_n} S_{\mathfrak{M}_n}^{1/2} \in \mathbb{R}^{mn \times d}$ and let $\mathbf{Z}_n := [\mathbf{X}_n^T | \mathbf{X}_n^T | \dots | \mathbf{X}_n^T]^T \in \mathbb{R}^{mn \times d}$. The quantity of interest is the h -th row of

$$n^{1/2} \left(\hat{\mathbf{X}}_{\mathfrak{M}_n} V_n^T W_n - \mathbf{Z}_n \right),$$

where $V_n, W_n \in \mathbb{R}^{d \times d}$ are suitable orthogonal transformations and W_n is such that $\mathbf{Z}_n = U_{\tilde{P}_n} S_{\tilde{P}_n}^{1/2} W_n$. This quantity can be decomposed into a sum of matrices (Eq. (31)) as (dropping the subscripted dependence on n)

$$\begin{aligned} n^{1/2} \left(U_{\mathfrak{M}} S_{\mathfrak{M}}^{1/2} - U_{\tilde{P}} S_{\tilde{P}}^{1/2} V \right)_h V^T W &= n^{1/2} \left((\mathfrak{M} - \tilde{P}) U_{\tilde{P}} S_{\tilde{P}}^{-1/2} V \right)_h V^T W + (n^{1/2} R_h V) V^T W \\ &= n^{1/2} \left((\mathfrak{M} - \tilde{P}) U_{\tilde{P}} S_{\tilde{P}}^{-1/2} W \right)_h + n^{1/2} R_h W, \end{aligned}$$

where $R_h \in \mathbb{R}^{mn \times d}$ is the residual matrix. As a consequence of the consistency of the omnibus estimates illustrated in Theorem 5, we obtain that the rows of the matrix $n^{1/2} R_h$ converge in probability to 0. Next, Lemma 6 establishes that

$$n^{1/2} \left((\mathfrak{M} - \tilde{P}) U_{\tilde{P}} S_{\tilde{P}}^{-1/2} W \right)_h$$

converges in distribution to a mixture of normals, and by applying Slutsky's Theorem the proof of Theorem 3 is complete.

A.3 General omnibus consistency

Theorem 5 (Consistency of omnibus estimates). *With notation as in Theorem 3, assume that F is such that if $X \sim F$, then $\mathbb{E}(XX^T)$ is rank d . Then there exists an orthogonal matrix $V \in \mathcal{O}_d$ and a constant $C > 0$ such that, with high probability,*

$$\|U_{\mathfrak{M}} S_{\mathfrak{M}}^{1/2} - U_{\tilde{P}} S_{\tilde{P}}^{1/2} V\|_{2 \rightarrow \infty} \leq C \frac{m^{3/2} \log^{1/2} mn}{n^{1/2}}.$$

To prove Theorem 5, we will need a number of intermediate supporting lemmas (Lemmas 2–7), including a Bernstein concentration inequality bound given in subsection A.3.2, all of which are suitably adapted from [26].

A.3.1 Supporting Lemmas

Lemma 2 (Observation 2 in [26]). *Let F be a distribution on a set $\mathcal{X} \in \mathbb{R}^d$ satisfying $\langle x, x' \rangle \in [0, 1]$ for all $x, x' \in \mathcal{X}$. Let $X_1, X_2, \dots, X_n, Y \stackrel{i.i.d.}{\sim} F$, and let $P = \mathbf{X}\mathbf{X}^T$ where $\mathbf{X} = [X_1^T | X_2^T | \dots | X_n^T]^T$. Then with probability at least $1 - \frac{d^2}{n^2}$, we have that*

$$|\lambda_i(P) - n\lambda_i\mathbb{E}(YY^T)| \leq 2d\sqrt{n \log n}.$$

Furthermore, with high probability there exists a constant $C > 0$ such that for all $i \in [d]$, $\lambda_i(P) \geq Cn\delta$ and $\lambda_i(\tilde{P}) \geq Cnm\delta$, where $\delta = \lambda_d(\mathbb{E}(YY^T))$.

Combining Lemma 2 with the fact that the rows of $U_{\tilde{P}} S_{\tilde{P}}^{1/2}$ are bounded in Euclidean norm by 1, we obtain

$$\|U_{\tilde{P}}\|_{2 \rightarrow \infty} \leq C(mn)^{-1/2} \text{ w.h.p.} \quad (24)$$

Lemma 3. *With notation as in Lemma 2, assume that $\delta > 0$ so that $\mathbb{E}(YY^T)$ is full rank. Let the singular value decomposition of $U_{\tilde{P}}^T U_{\mathfrak{M}} \in \mathbb{R}^{d \times d}$ be given by $V_1 \Sigma V_2^T$. Then, there exists a constant $C > 0$ such that*

$$\|U_{\tilde{P}}^T U_{\mathfrak{M}} - V_1 V_2^T\|_F \leq \frac{Cm \log mn}{n} \quad w.h.p.$$

Adapted from the proof of Proposition 16 in [33]. Working on the intersection of the sets where both Lemma 5 and 2 hold (noting this set has high probability), note that Weyl's theorem gives that $\lambda_d(\mathfrak{M}) \geq Cnm$ for some constant C . Let $\sigma_1 \geq \sigma_2 \geq \dots \geq \sigma_d$ be the singular values of $U_{\tilde{P}}^T U_{\mathfrak{M}}$, so that $\sigma_i = \cos(\theta_i)$ where the θ_i 's are the principal angles between the subspaces spanned by $U_{\tilde{P}}$ and $U_{\mathfrak{M}}$. The Davis-Kahan theorem (see, for example, Theorem 3.6 in [6] Theorem VII.3.1) then implies that with high probability (where C is a constant that can change line-to-line)

$$\begin{aligned} \|U_{\tilde{P}}^T U_{\mathfrak{M}} - V_1 V_2^T\|_F &= \sqrt{\sum_i (1 - \sigma_i)^2} \\ &\leq \sum_i (1 - \sigma_i^2) \\ &\leq d \max_i |\sin(\theta_i)|^2 \\ &\leq \frac{Cd^2 \|\mathfrak{M} - \tilde{P}\|^2}{\lambda_d(\mathfrak{M})^2} \\ &\leq \frac{Cm^3(n-1) \log mn}{n^2 m^2} \\ &\leq \frac{Cm \log mn}{n}, \end{aligned}$$

where the bounds in the fourth line follows from Davis-Kahan, and those in the second-to-last line follow from Lemma 5 (numerator) and Lemma 2 (denominator). \square

Lemma 4. *With the assumptions and notation of Lemma 3, let $V = V_1 V_2^T$. Then we have that*

$$\|V S_{\mathfrak{M}} - S_{\tilde{P}} V\|_F \leq C m^2 \log mn \quad w.h.p. \quad (25)$$

$$\|V S_{\mathfrak{M}}^{1/2} - S_{\tilde{P}}^{1/2} V\|_F \leq C \frac{m^{3/2} \log mn}{n^{1/2}} \quad w.h.p. \quad (26)$$

$$\|V S_{\mathfrak{M}}^{-1/2} - S_{\tilde{P}}^{-1/2} V\|_F \leq C \frac{m^{1/2} \log mn}{n^{3/2}} \quad w.h.p. \quad (27)$$

(where $S_{\mathfrak{M}}^{-1}$, and $S_{\tilde{P}}^{-1}$ are understood to be the pseudoinverses of $S_{\mathfrak{M}}$, and $S_{\tilde{P}}$ in the unlikely event these matrices are singular).

Proof: Adapted from the proof of Proposition 17 in [33]. Let

$$R := U_{\mathfrak{M}} - U_{\tilde{P}} U_{\tilde{P}}^T U_{\mathfrak{M}},$$

so that

$$\begin{aligned} V S_{\mathfrak{M}} &= (V - U_{\tilde{P}}^T U_{\mathfrak{M}}) S_{\mathfrak{M}} + U_{\tilde{P}}^T U_{\mathfrak{M}} S_{\mathfrak{M}} \\ &= (V - U_{\tilde{P}}^T U_{\mathfrak{M}}) S_{\mathfrak{M}} + U_{\tilde{P}}^T \mathfrak{M} U_{\mathfrak{M}} I_{\pm} \\ &= (V - U_{\tilde{P}}^T U_{\mathfrak{M}}) S_{\mathfrak{M}} + U_{\tilde{P}}^T (\mathfrak{M} - \tilde{P}) U_{\mathfrak{M}} I_{\pm} + U_{\tilde{P}}^T \tilde{P} U_{\mathfrak{M}} I_{\pm} \\ &= (V - U_{\tilde{P}}^T U_{\mathfrak{M}}) S_{\mathfrak{M}} + U_{\tilde{P}}^T (\mathfrak{M} - \tilde{P}) R I_{\pm} + U_{\tilde{P}}^T (\mathfrak{M} - \tilde{P}) U_{\tilde{P}} U_{\tilde{P}}^T U_{\mathfrak{M}} I_{\pm} + U_{\tilde{P}}^T \tilde{P} U_{\mathfrak{M}} I_{\pm} \\ &= (V - U_{\tilde{P}}^T U_{\mathfrak{M}}) S_{\mathfrak{M}} + U_{\tilde{P}}^T (\mathfrak{M} - \tilde{P}) R I_{\pm} + U_{\tilde{P}}^T (\mathfrak{M} - \tilde{P}) U_{\tilde{P}} U_{\tilde{P}}^T U_{\mathfrak{M}} I_{\pm} + S_{\tilde{P}} U_{\tilde{P}}^T U_{\mathfrak{M}} I_{\pm}, \end{aligned}$$

where I_{\pm} is a random diagonal matrix with ± 1 entries on its diagonal indicating whether the signs of the eigenvalues associated with $U_{\mathfrak{M}}$ agree for \mathfrak{M} and for $|\mathfrak{M}|$.

We will first bound the Frobenius norm of $U_{\tilde{P}}^T (\mathfrak{M} - \tilde{P}) U_{\tilde{P}}$. The i, j -th entry of $U_{\tilde{P}}^T (\mathfrak{M} - \tilde{P}) U_{\tilde{P}} \in \mathbb{R}^{d \times d}$ is of the form (where u_i is the i -th column of $U_{\tilde{P}}$)

$$\begin{aligned} u_i^T (\mathfrak{M} - \tilde{P}) u_j &= \sum_{k, \ell=1}^m (\mathfrak{M}_{k, \ell} - \tilde{P}_{k, \ell}) u_{ki} u_{\ell j} \\ &= 2 \sum_{k < \ell} (\mathfrak{M}_{k, \ell} - \tilde{P}_{k, \ell}) u_{ki} u_{\ell j} - \sum_k \tilde{P}_{k, k} u_{ki} u_{kj} \end{aligned}$$

Conditioning on \mathbf{X} (and hence on P), we have that $2 \sum_{k < \ell} (\mathfrak{M}_{k, \ell} - \tilde{P}_{k, \ell}) u_{ki} u_{\ell j}$ is a mean zero random variable and is a function of $m \binom{n}{2}$ independent Bernoulli random variables (the $\{A_{\alpha, \beta}^{(h)}\}_{h, \alpha, \beta}$). If $\tilde{\mathfrak{M}}$ is \mathfrak{M} computed with one Bernoulli (say $A_{\alpha, \beta}^{(h)}$) flipped, then note that

- If $\alpha, \beta \in [n]$ are such that $\{k, \ell\} \equiv \{\alpha, \beta\} \pmod{n}$, then we can write $\mathfrak{M}_{k, \ell}$ as

$$\mathfrak{M}_{k, \ell} = \sum_h c_h^{(\lceil k/n \rceil, \lceil \ell/n \rceil)} A_{\alpha, \beta}^{(h)}.$$

Therefore

$$|\mathfrak{M}_{k, \ell} - \tilde{\mathfrak{M}}_{k, \ell}| \leq c_h^{(\lceil k/n \rceil, \lceil \ell/n \rceil)}$$

- If $\alpha, \beta \in [n]$ are such that $\{k, \ell\} \not\equiv \{\alpha, \beta\} \pmod{n}$, then $\mathfrak{M}_{k, \ell} = \tilde{\mathfrak{M}}_{k, \ell}$.

Therefore changing $A_{\alpha, \beta}^{(h)}$ can change the value of $2 \sum_{k < \ell} (\mathfrak{M}_{k, \ell} - \tilde{P}_{k, \ell}) u_{ki} u_{\ell j}$ by at most

$$\begin{aligned} &|2 \sum_{k < \ell} (\tilde{\mathfrak{M}}_{k, \ell} - \tilde{P}_{k, \ell}) u_{ki} u_{\ell j} - 2 \sum_{k < \ell} (\mathfrak{M}_{k, \ell} - \tilde{P}_{k, \ell}) u_{ki} u_{\ell j}| \\ &\leq 2 \sum_{\substack{k < \ell \\ \{k, \ell\} \equiv \{\alpha, \beta\} \pmod{n}}} |c_h^{(\lceil k/n \rceil, \lceil \ell/n \rceil)}| |u_{ki}| |u_{\ell j}| \\ &\leq 2 \sum_{\substack{k < \ell \\ \{k, \ell\} \equiv \{\alpha, \beta\} \pmod{n}}} |u_{ki}| \cdot |u_{\ell j}| := c_{h, \alpha, \beta} \end{aligned}$$

Therefore, the total amount of possible change (the denominator in the McDiarmid bound exponent) is bounded via

$$\begin{aligned}
\sum_{h=1}^m \sum_{\alpha=1}^n \sum_{\beta=1}^n c_{h,\alpha,\beta}^2 &= 4 \sum_{h=1}^m \sum_{\alpha=1}^n \sum_{\beta=1}^n \left(\sum_{\substack{k < \ell \\ \{k,\ell\} \equiv \{\alpha,\beta\} \pmod{n}}} |u_{ki}| \cdot |u_{\ell j}| \right)^2 \\
&\stackrel{C.S. \neq}{\leq} 8m^2 \sum_{h=1}^m \sum_{\alpha=1}^n \sum_{\beta=1}^n \sum_{\substack{k < \ell \\ \{k,\ell\} \equiv \{\alpha,\beta\} \pmod{n}}} |u_{ki}|^2 \cdot |u_{\ell j}|^2 \\
&\leq 8m^2 \sum_{h=1}^m \sum_{\alpha=1}^n \sum_{\beta=1}^n \left(\sum_{\substack{k < \ell \\ k \equiv \alpha \pmod{n} \\ \ell \equiv \beta \pmod{n}}} |u_{ki}|^2 \cdot |u_{\ell j}|^2 + \sum_{\substack{k < \ell \\ k \equiv \beta \pmod{n} \\ \ell \equiv \alpha \pmod{n}}} |u_{ki}|^2 \cdot |u_{\ell j}|^2 \right) \\
&\leq 8m^2 \sum_{h=1}^m \sum_{\alpha=1}^n \sum_{\beta=1}^n \left(\sum_{k:k \equiv \alpha \pmod{n}} |u_{ki}|^2 \sum_{\ell:\ell \equiv \beta \pmod{n}} |u_{\ell j}|^2 + \sum_{k:k \equiv \beta \pmod{n}} |u_{ki}|^2 \sum_{\ell:\ell \equiv \alpha \pmod{n}} |u_{\ell j}|^2 \right) \\
&\leq 16m^3 \left(\sum_{\alpha=1}^n \sum_{k:k \equiv \alpha \pmod{n}} |u_{ki}|^2 \right) \left(\sum_{\beta=1}^n \sum_{\ell:\ell \equiv \beta \pmod{n}} |u_{\ell j}|^2 \right) = 16m^3
\end{aligned}$$

Therefore, McDiarmid's inequality implies that $2 \sum_{k < \ell} (\mathfrak{M}_{k,\ell} - \tilde{P}_{k,\ell}) u_{ki} u_{\ell j}$ is, w.h.p., of the order $O(m^2 \log mn)$. Noting that $|\sum_k \tilde{P}_{k,k} u_{ki} u_{kj}| \leq \sum_k |u_{ki} u_{kj}| \leq \|u_i\|_2 \|u_j\|_2 = 1$, we have $u_i^T (\mathfrak{M} - \tilde{P}) u_j$ is, w.h.p., $O(m^2 \log mn)$. Further, applying the Frobenius norm to $d \times d$ matrix $U_{\tilde{P}}^T (\mathfrak{M} - \tilde{P}) U_{\tilde{P}}$, and integrating over the possible \mathbf{X} , we get that with high probability, there exists a constant C such that

$$\|U_{\tilde{P}}^T (\mathfrak{M} - \tilde{P}) U_{\tilde{P}}\|_F \leq C m^2 \log mn. \quad (28)$$

Consider the events (where C is an appropriately chosen constant)

$$\begin{aligned}
\mathcal{E}_1 &:= \left\{ \|U_{\tilde{P}}^T (\mathfrak{M} - \tilde{P}) U_{\tilde{P}}\|_F \leq C m^2 \log mn \right\} \\
\mathcal{E}_2 &:= \{ \text{the statement of Lemma 2 holds} \} \\
\mathcal{E}_3 &:= \{ \text{the statement of Lemma 3 holds} \} \\
\mathcal{E}_4 &:= \{ \text{the statement of Lemma 5 holds} \}
\end{aligned}$$

As each \mathcal{E}_i is a high probability event, $\mathcal{E} = \cap_{i=1}^4 \mathcal{E}_i$ is also a high probability event. In what follows, we will condition on the events in \mathcal{E} occurring.

Conditioning on \mathcal{E} , we have that from the Davis-Kahan theorem,

$$\|U_{\mathfrak{M}} - U_{\tilde{P}} U_{\tilde{P}}^T U_{\mathfrak{M}}\| \leq \sqrt{\frac{C m \log mn}{n}}$$

holds for some constant C . Also, Weyl's theorem [24, Section 6.3] with Lemmas 2 and 5 imply that

$$|\lambda_j(\mathfrak{M})| \leq C m^{3/2} \sqrt{n \log mn}$$

for $j > d$, and that

$$|\lambda_j(\mathfrak{M}) - \lambda_j(\tilde{P})| \leq Cm^{3/2}\sqrt{n \log mn}$$

$j \leq d$. As for $j \leq d$, we have that there is a constant $C > 0$ such that $\lambda_j(\tilde{P}) \geq Cnm\delta$, and so $\lambda_i(|\mathfrak{M}|) = \lambda_i(\mathfrak{M}) \geq Cnm\delta$ for all $i \in [d]$ and an appropriately chosen constant C (abusing notation, the two C 's need not be equal). Therefore, we have that $I_{\pm} = I_d$ so that

$$S_{\tilde{P}}U_{\tilde{P}}^TU_{\mathfrak{M}}I_{\pm} = S_{\tilde{P}}U_{\tilde{P}}^TU_{\mathfrak{M}} = S_{\tilde{P}}(U_{\tilde{P}}^TU_{\mathfrak{M}} - V) + S_{\tilde{P}}V.$$

We have then that

$$\begin{aligned} \|VS_{\mathfrak{M}} - S_{\tilde{P}}V\|_F &\leq \|V - U_{\tilde{P}}^TU_{\tilde{P}}\|_F(\|S_{\mathfrak{M}}\| + \|S_{\tilde{P}}\|) \\ &\quad + \|U_{\tilde{P}}^T(\mathfrak{M} - \tilde{P})R\|_F + \|U_{\tilde{P}}^T(\mathfrak{M} - \tilde{P})U_{\tilde{P}}U_{\tilde{P}}^TU_{\mathfrak{M}}\|_F \end{aligned}$$

Now, we have that $\|\mathfrak{M}\|, \|\tilde{P}\| \leq mn$. It follows then that there exists a constant C such that

$$\begin{aligned} \|V - U_{\tilde{P}}^TU_{\tilde{P}}\|_F(\|S_{\mathfrak{M}}\| + \|S_{\tilde{P}}\|) &\leq Cm^2 \log mn \\ \|U_{\tilde{P}}^T(\mathfrak{M} - \tilde{P})R\|_F &\leq \sqrt{d}\|U_{\tilde{P}}^T(\mathfrak{M} - \tilde{P})R\| \leq Cm^2 \log mn \end{aligned}$$

so that

$$\|VS_{\mathfrak{M}} - S_{\tilde{P}}V\|_F \leq Cm^2 \log mn + \|U_{\tilde{P}}^T(\mathfrak{M} - \tilde{P})U_{\tilde{P}}\|_F \leq Cm^2 \log mn.$$

as desired, thus proving Eq. (25).

To prove Eq. (26) and (27), note that we have shown that with high probability, both of the following events hold:

- i. $\|VS_{\mathfrak{M}} - S_{\tilde{P}}V\|_F \leq Cm^2 \log mn$ (by the first part of the Lemma)
- ii. For all $i, j \in [d]$, $\lambda_i(\mathfrak{M}), \lambda_j(\tilde{P})$ are of order $\Omega(nm\delta)$ (by Lemmas 2 and 5).

Given these events, as we have that

$$(S_{\mathfrak{M}}^{1/2} - S_{\tilde{P}}^{1/2})(S_{\mathfrak{M}}^{1/2} + S_{\tilde{P}}^{1/2}) = (S_{\mathfrak{M}} - S_{\tilde{P}}) \Rightarrow (S_{\mathfrak{M}}^{1/2} - S_{\tilde{P}}^{1/2}) = (S_{\mathfrak{M}} - S_{\tilde{P}})(S_{\mathfrak{M}}^{1/2} + S_{\tilde{P}}^{1/2})^{-1},$$

the i, j -th entry of $V S_{\mathfrak{M}}^{1/2} - S_{\tilde{P}}^{1/2}V$ is equal to

$$V_{i,j}(\lambda_i^{1/2}(\mathfrak{M}) - \lambda_j^{1/2}(\tilde{P})) = \frac{V_{i,j}(\lambda_i(\mathfrak{M}) - \lambda_j(\tilde{P}))}{\lambda_i^{1/2}(\mathfrak{M}) + \lambda_j^{1/2}(\tilde{P})}$$

and Eq. (26) follows. To prove Eq. (27), note that the i, j -th entry of $V S_{\mathfrak{M}}^{-1/2} - S_{\tilde{P}}^{-1/2}V$ is equal to

$$V_{i,j}(\lambda_i^{-1/2}(\mathfrak{M}) - \lambda_j^{-1/2}(\tilde{P})) = \frac{V_{i,j}(\lambda_j(\tilde{P})^{1/2} - \lambda_i(\mathfrak{M})^{1/2})}{\sqrt{\lambda_i(\mathfrak{M})\lambda_j(\tilde{P})}}$$

The proof then follows immediately. \square

A.3.2 Concentration inequality via matrix Bernstein

Lemma 5. *With the assumptions in Lemma 3, there exists a constant $C > 0$ such that, with high probability,*

$$\|\mathfrak{M} - \mathbb{E} \mathfrak{M}\| \leq Cm \sqrt{\tilde{L}(n-1) \log mn} \leq Cm^{3/2} \sqrt{(n-1) \log mn},$$

where $\tilde{L} = \max_{\ell} \max_{ij} \sum_{k=1}^m c_{\ell}^{(i,k)} c_{\ell}^{(j,k)}$ and $C > 0$ a fixed constant.

Proof. Condition on \mathbf{X} and let $P = \mathbf{X}\mathbf{X}^T$, so that

$$\mathbb{E} \mathfrak{M} = \tilde{P} = \begin{bmatrix} P & P & \cdots & P \\ P & P & \cdots & P \\ \vdots & \vdots & \ddots & \vdots \\ P & P & \cdots & P \end{bmatrix}.$$

For all $l \in [m]$ and $i, j \in [n]$, we define an auxiliary block matrix $E_{i,j}^{(l)} \in \mathbb{R}^{mn \times mn}$ which will help us express the difference $\mathfrak{M} - \mathbb{E} \mathfrak{M}$ as a sum of independent Hermitian matrices, which will allow us to apply Bernstein's matrix bound (see, for example, Theorem 5.4.1 in [50]). For $i \neq j$, let $e^{ij} = e_i e_j^T + e_j e_i^T$ where e_i is a vector in \mathbb{R}^n with all its entries equal to 0 except the i -th entry which is equal to 1, so that e^{ij} is a matrix whose entries are all equal to 0 except the (i, j) th and (j, i) th entries which are equal to 1. For $\ell \in [m]$, we define the $m \times m$ matrix $C^{(\ell)}$ (symmetric because \mathfrak{M} is symmetric) as follows,

$$C^{(\ell)} = \begin{bmatrix} c_{\ell}^{(1,1)} & c_{\ell}^{(1,2)} & \cdots & c_{\ell}^{(1,m)} \\ c_{\ell}^{(2,1)} & c_{\ell}^{(2,2)} & \cdots & c_{\ell}^{(2,m)} \\ \vdots & \vdots & \ddots & \vdots \\ c_{\ell}^{(m,1)} & c_{\ell}^{(m,2)} & \cdots & c_{\ell}^{(m,m)} \end{bmatrix}.$$

We then define the $mn \times mn$ block (symmetric) matrix $E_{i,j}^{(\ell)}$ as the Kronecker product of $C^{(\ell)}$ and e^{ij} , i.e., $E_{i,j}^{(\ell)} = C^{(\ell)} \otimes e^{ij}$. Now, we can write $\mathfrak{M} - \mathbb{E} \mathfrak{M}$ as

$$\mathfrak{M} - \mathbb{E} \mathfrak{M} = \sum_{1 \leq \ell \leq m} \sum_{1 \leq i < j \leq n} (A_{ij}^{(\ell)} - P_{ij}) E_{i,j}^{(\ell)}$$

which is a sum of $m \binom{n}{2}$ independent zero-mean matrices (the $(A_{ij}^{(\ell)} - P_{ij}) E_{i,j}^{(\ell)}$), with

$$\|(A_{ij}^{(\ell)} - P_{ij}) E_{i,j}^{(\ell)}\| \leq \|C^{(\ell)}\| \leq \max_{\ell \in [m]} \max_{i \in [m]} \sum_{j=1}^m c_{\ell}^{(i,j)}$$

for all $\ell \in [m]$ and $i, j \in [n]$.

To apply the matrix Bernstein inequality, it remains to compute the variance term

$$\nu(\mathfrak{M} - \mathbb{E} \mathfrak{M}) = \left\| \sum_{1 \leq \ell \leq m} \sum_{1 \leq i < j \leq n} \mathbb{E} \left[(A_{ij}^{(\ell)} - P_{ij})^2 (E_{i,j}^{(\ell)})^2 \right] \right\|.$$

Let $D_{ij} = e^{ij}e^{ij} = e_i e_i^T + e_j e_j^T \in \mathbb{R}^{n \times n}$. From the mixed-product property of Kronecker matrix multiplication, we have that

$$E_{i,j}^{(\ell)} E_{i,j}^{(\ell)} = (C^{(\ell)} \otimes e^{ij})(C^{(\ell)} \otimes e^{ij}) = (C^{(\ell)})^2 \otimes D_{ij}.$$

Note that for any symmetric matrix A , we have that $\|A\| \leq \sqrt{\|A\|_1 \|A\|_\infty} = \|A\|_\infty$ (see, for example, [24] Ex. 5.6.21), where $\|\cdot\|_1$ is the maximum column sum matrix norm and $\|\cdot\|_\infty$ the maximum row sum matrix norm. We then have

$$\begin{aligned} \nu(\mathfrak{M} - \mathbb{E} \mathfrak{M}) &= \left\| \sum_{1 \leq \ell \leq m} \sum_{1 \leq i < j \leq n} P_{ij}(1 - P_{ij}) E_{i,j}^{(\ell)} E_{i,j}^{(\ell)} \right\| \\ &\leq \left\| \sum_{1 \leq \ell \leq m} \sum_{1 \leq i < j \leq n} P_{ij}(1 - P_{ij}) [(C^{(\ell)})^2 \otimes D_{ij}] \right\|_\infty \\ &\leq (n-1)m^2 \max_{\ell \in [m]} \max_{i,j \in [n]} \sum_{k=1}^m c_\ell^{(i,k)} c_\ell^{(j,k)}. \end{aligned}$$

Let

$$\begin{aligned} L &:= \max_{\ell \in [m]} \max_{i \in [m]} \sum_{j=1}^m c_\ell^{(i,j)} \leq m; \\ \tilde{L} &:= \max_{\ell \in [m]} \max_{i,j \in [n]} \sum_{k=1}^m c_\ell^{(i,k)} c_\ell^{(j,k)} \leq L \end{aligned}$$

To apply Bernstein's bound, let $t = 4m\sqrt{\tilde{L}(n-1)\log mn}$, and then

$$\begin{aligned} \mathbb{P} \left[\|\mathfrak{M} - \mathbb{E} \mathfrak{M}\| \geq 4m\sqrt{\tilde{L}(n-1)\log mn} \right] &\leq 2nm \cdot \exp \left\{ \frac{-8m^2 \tilde{L}(n-1)\log mn}{\nu(\mathfrak{M} - \mathbb{E} \mathfrak{M}) + \frac{4mL\sqrt{\tilde{L}(n-1)\log mn}}{3}} \right\} \\ &\leq 2nm \cdot \exp \left\{ \frac{-8m^2 \tilde{L}(n-1)\log mn}{(n-1)m^2 \tilde{L} + \frac{4mL\sqrt{\tilde{L}(n-1)\log mn}}{3}} \right\} \\ &\leq 2nm \cdot \exp \left\{ \frac{-8m^2 \tilde{L}(n-1)\log mn}{2(n-1)m^2 \tilde{L}} \right\} \\ &= 2m^{-3}n^{-3}, \end{aligned}$$

where the third inequality holds for n sufficiently large. Integrating over the \mathbf{X} then yields the desired result.

A.3.3 Supporting lemmas

Before proving our main results, we first state and prove a pair of intermediate lemmas.

Lemma 6. *With the assumptions in Lemma 3, denote the SVD of $U_{\tilde{P}}^T U_{\mathfrak{M}}$ as $V_1 \Sigma V_2^T$ and set $V := V_1 V_2^T$. There exists a constant C such that w.h.p.*

$$\|(\mathfrak{M} - \tilde{P})U_{\tilde{P}}\|_{2 \rightarrow \infty} \leq C\sqrt{dm}\sqrt{\log mn}. \quad (29)$$

Proof. We note first that

$$\frac{1}{\sqrt{d}} \|(\mathfrak{M} - \tilde{P})U_{\tilde{P}}\|_{2 \rightarrow \infty} \leq \|(\mathfrak{M} - \tilde{P})U_{\tilde{P}}\|_{\max} = \max_{i \in [mn], j \in [d]} |\langle (\mathfrak{M} - \tilde{P})U_{\cdot,j}, e_i \rangle|,$$

where $e_i \in \mathbb{R}^{mn}$ is the unit vector with all of its entries equal to 0, except for the i -th entry.

Let $s \in [m]$ arbitrary. There exists a matrix W such that

$$U_{\tilde{P}} S_{\tilde{P}}^{1/2} W = \mathbf{Z} \Rightarrow U_{\tilde{P}} = \mathbf{Z} W^T (S_{\tilde{P}})^{-1/2} = \begin{bmatrix} \mathbf{X} W^T (S_{\tilde{P}})^{-1/2} \\ \mathbf{X} W^T (S_{\tilde{P}})^{-1/2} \\ \vdots \\ \mathbf{X} W^T (S_{\tilde{P}})^{-1/2} \end{bmatrix}.$$

Therefor, for all $1 \leq k \leq n$, $U_{k,j} = U_{k+n,j} = \dots = U_{k+(m-1)n,j}$. For each $(s-1)n+1 \leq i \leq sn$ and $1 \leq j \leq d$,

$$\begin{aligned} \langle (\mathfrak{M} - \tilde{P})U_{\cdot,j}, e_i \rangle &= e_i^T (\mathfrak{M} - \tilde{P})U_{\cdot,j} \\ &= \sum_{\tilde{k}=1}^{mn} (\mathfrak{M}_{i,\tilde{k}} - \tilde{P}_{i,\tilde{k}}) U_{\tilde{k},j} \\ &= \sum_{k=1}^n \left[\sum_{t=1}^m \mathfrak{M}_{i,k}^{(s,t)} - m P_{i,k} \right] U_{k,j} \\ &= \sum_{k=1}^n \left[\sum_{t=1}^m \sum_{\ell=1}^m c_{\ell}^{(s,t)} A_{i,k}^{(\ell)} - m P_{i,k} \right] U_{k,j} \\ &= \sum_{k=1}^n \left[\sum_{\ell=1}^m \alpha(s, \ell) A_{i,k}^{(\ell)} - m P_{i,k} \right] U_{k,j}, \end{aligned} \tag{30}$$

where $\alpha(s, \ell) := \sum_{t=1}^m c_{\ell}^{(s,t)} \geq 0$ and $\sum_{\ell=1}^m \alpha(s, \ell) = m$ for all $s \in [m]$. For all $s \in [m]$, for any $(s-1)n+1 \leq i \leq sn$ and $1 \leq j \leq d$, the above expansion is a sum of n independent (in k), bounded, mean zero random variables taking values in $[-mU_{k,j}, mU_{k,j}]$. Hence, by Hoeffding's inequality,

$$\mathbb{P} \left(\left| \sum_{\tilde{k}=1}^{mn} (\mathfrak{M}_{i,\tilde{k}} - \tilde{P}_{i,\tilde{k}}) U_{\tilde{k},j} \right| \geq 2m\sqrt{\log mn} \right) \leq 2 \exp \left(- \frac{8m^2 \log mn}{\sum_{k=1}^n (2mU_{k,j})^2} \right) \leq 2(mn)^{-2},$$

where we used the fact that $\sum_{k=1}^n (2mU_{k,j})^2 \leq 4m^2$ as the columns of $U_{\tilde{P}}$ are norm 1. Therefore, w.h.p. there exists a constant $C > 0$ such that $\|(\mathfrak{M} - \tilde{P})U_{\tilde{P}}\|_{2 \rightarrow \infty} \leq C\sqrt{d}m\sqrt{\log mn}$ as desired. \square

Lemma 7. *With the assumptions in Lemma 3, denote the SVD of $U_{\tilde{P}}^T U_{\mathfrak{M}}$ as $V_1 \Sigma V_2^T$ and set $V := V_1 V_2^T$. Set also $Q^{(1)} = U_{\mathfrak{M}} - U_{\tilde{P}} V$, there exists a constant C such that w.h.p.,*

$$\|Q^{(1)}\| \leq C \frac{m^{1/2} \log^{1/2} mn}{n^{1/2}}$$

Proof. Following the reasoning from Lemma 6.8 in [8], we add and subtract $U_{\tilde{P}}U_{\tilde{P}}^TU_{\mathfrak{M}}$ and by triangle inequality,

$$\|Q^{(1)}\| = \|U_{\mathfrak{M}} - U_{\tilde{P}}V\| \leq \|U_{\mathfrak{M}} - U_{\tilde{P}}U_{\tilde{P}}^TU_{\mathfrak{M}}\| + \|U_{\tilde{P}}(U_{\tilde{P}}^TU_{\mathfrak{M}} - V)\|.$$

The first term can be rewritten as follows,

$$\|U_{\mathfrak{M}} - U_{\tilde{P}}U_{\tilde{P}}^TU_{\mathfrak{M}}\| = \|U_{\mathfrak{M}}U_{\mathfrak{M}}^T - U_{\tilde{P}}U_{\tilde{P}}^TU_{\mathfrak{M}}U_{\mathfrak{M}}^T\| = \|(I - U_{\tilde{P}}U_{\tilde{P}}^T)U_{\mathfrak{M}}U_{\mathfrak{M}}^T\| = \|\sin \Theta(U_{\mathfrak{M}}, U_{\tilde{P}})\|$$

Given the intersection of the events in the statements of Lemmas 2 and 5, the Davis-Kahan theorem gives that,

$$\|U_{\mathfrak{M}} - U_{\tilde{P}}U_{\tilde{P}}^TU_{\mathfrak{M}}\| \leq \frac{\|\mathfrak{M} - \tilde{P}\|}{\lambda_d(\mathfrak{M})} \leq C \frac{m^{1/2} \log^{1/2} mn}{n^{1/2}}$$

Further, we can bound $\|U_{\tilde{P}}(U_{\tilde{P}}^TU_{\mathfrak{M}} - V)\|$ using Lemma 3; as the intersection of the events in Lemma 2, 3 and 5 has high probability, this leads us to the desired result. \square

Proof of Theorem 5. Let W_n be a sequence of matrices such that $\mathbf{Z} = \mathbf{Z}^*W_n$, and let V be as in Lemma 4. Define the matrices $Q^{(1)}, Q^{(2)}$ as follows

$$\begin{aligned} Q^{(1)} &= U_{\mathfrak{M}} - U_{\tilde{P}}V; \\ Q^{(2)} &= U_{\tilde{P}}U_{\tilde{P}}^TU_{\mathfrak{M}} - U_{\tilde{P}}V. \end{aligned}$$

Note that, as defined, $\mathfrak{M}U_{\mathfrak{M}} = S_{\mathfrak{M}}I_{\pm}$ where I_{\pm} is a random sign matrix indicating whether the signs of the eigenvalues associated with $U_{\mathfrak{M}}$ agree for \mathfrak{M} and $|\mathfrak{M}|$. Given the events of Lemmas 2 and 5, we have that (by Weyl's Theorem) $I_{\pm} = I_d$; as this term appears only in the residual terms (H_2 - H_5) of the below decomposition, and as, when bounding the residual terms we assume the events of Lemmas 2 and 5, we (slightly abusing notation) write $\mathfrak{M}U_{\mathfrak{M}} = S_{\mathfrak{M}}$ in the below decomposition. We decompose the term $U_{\mathfrak{M}}S_{\mathfrak{M}}^{1/2} - U_{\tilde{P}}S_{\tilde{P}}^{1/2}V$ as follows,

$$\begin{aligned} U_{\mathfrak{M}}S_{\mathfrak{M}}^{1/2} - U_{\tilde{P}}S_{\tilde{P}}^{1/2}V &= \underbrace{(\mathfrak{M} - \tilde{P})U_{\tilde{P}}S_{\tilde{P}}^{-1/2}V}_{:=H_1} + \underbrace{(\mathfrak{M} - \tilde{P})U_{\tilde{P}}(VS_{\mathfrak{M}}^{-1/2} - S_{\tilde{P}}^{-1/2}V)}_{:=H_2} \\ &\quad - \underbrace{U_{\tilde{P}}U_{\tilde{P}}^T(\mathfrak{M} - \tilde{P})U_{\tilde{P}}VS_{\mathfrak{M}}^{-1/2}}_{:=H_3} + \underbrace{(I - U_{\tilde{P}}U_{\tilde{P}}^T)(\mathfrak{M} - \tilde{P})Q^{(1)}S_{\mathfrak{M}}^{-1/2}}_{:=H_4} \\ &\quad + \underbrace{Q^{(2)}S_{\mathfrak{M}}^{1/2} + U_{\tilde{P}}(VS_{\mathfrak{M}}^{1/2} - S_{\tilde{P}}^{1/2}V)}_{:=H_5} \end{aligned} \tag{31}$$

Here, H_4 presents a deviation from the proof in the standard omnibus setting (indeed, we cannot utilize the exchangeability they employ to bound H_4). For the H_i 's, $i = 1, 3$, there

exists a constant $C > 0$ such that the following bounds hold w.h.p.:

$$\begin{aligned}
\|H_1\|_{2 \rightarrow \infty} &\leq \|S_{\tilde{P}}^{-1/2}\| \cdot \|(\mathfrak{M} - \tilde{P})U_{\tilde{P}}\|_{2 \rightarrow \infty} \\
&\leq C \frac{m^{1/2} \log^{1/2} mn}{n^{1/2}} \quad [\text{Lemmas 2, 6}] \\
\|H_2\|_{2 \rightarrow \infty} &\leq \|VS_{\mathfrak{M}}^{-1/2} - S_{\tilde{P}}^{-1/2}V\| \cdot \|(\mathfrak{M} - \tilde{P})U_{\tilde{P}}\|_{2 \rightarrow \infty} \\
&\leq C \frac{m^{3/2} \log^{3/2} mn}{n^{3/2}} \quad [\text{Lemmas 4, 6}] \\
\|H_3\|_{2 \rightarrow \infty} &\leq \|U_{\tilde{P}}\|_{2 \rightarrow \infty} \|U_{\tilde{P}}^T(\mathfrak{M} - \tilde{P})U_{\tilde{P}}\| \cdot \|S_{\mathfrak{M}}^{-1/2}\| \\
&\leq C \frac{m \log mn}{n} \quad [\text{Lemma 2; Eq. (24), (28)}] \\
\|H_4\|_{2 \rightarrow \infty} &\leq \|(I - U_{\tilde{P}}U_{\tilde{P}}^T)\|_{2 \rightarrow \infty} \|(\mathfrak{M} - \tilde{P})\| \|Q^{(1)}\| \|S_{\mathfrak{M}}^{-1/2}\| \\
&\leq C \frac{m^{3/2} \log mn}{n^{1/2}} \quad [\text{Lemmas 2, 5, 7}].
\end{aligned}$$

Next, by Lemmas 2, 3 and Eq. (24) we get

$$\|Q^{(2)} S_{\mathfrak{M}}^{1/2}\|_{2 \rightarrow \infty} \leq \|U_{\tilde{P}}\|_{2 \rightarrow \infty} \|U_{\tilde{P}}^T U_{\mathfrak{M}} - V\| \cdot \|S_{\mathfrak{M}}^{1/2}\| \leq \frac{Cm \log mn}{n}$$

and by Lemma 4 and Eq (24) we get

$$\|U_{\tilde{P}}(VS_{\mathfrak{M}}^{1/2} - S_{\tilde{P}}^{1/2}V)\|_{2 \rightarrow \infty} \leq \|U_{\tilde{P}}\|_{2 \rightarrow \infty} \|(VS_{\mathfrak{M}}^{1/2} - S_{\tilde{P}}^{1/2}V)\| \leq \frac{Cm \log mn}{n}.$$

Hence, by triangle inequality,

$$\|H_5\|_{2 \rightarrow \infty} \leq C \frac{m \log mn}{n}.$$

Plugging into Eq. (31) the bounds above, then for sufficiently large n , applying triangle inequality yields the desired result.

A.4 Central limit theorem

Recall that, by the definition of the JRDPG, the latent positions of the expected omnibus matrix $\mathbb{E} \mathfrak{M} = \tilde{P} = U_{\tilde{P}} S_{\tilde{P}} U_{\tilde{P}}^T$ are given by

$$Z^* = \begin{bmatrix} X^* \\ X^* \\ \vdots \\ X^* \end{bmatrix} = U_{\tilde{P}} S_{\tilde{P}}^{1/2} \in \mathbb{R}^{mn \times d}$$

Recall that the matrix of the true latent positions is denoted by $Z = [X^T X^T \cdots X^T]^T \in \mathbb{R}^{mn \times d}$, so that $Z = Z^* W$ for some suitable-chosen orthogonal matrix W .

Theorem 6. *With notation and assumptions as in Theorem 3, fix some $i \in [n]$ and some $s \in [m]$ and let $h = n(s-1) + i$. Conditional on $X_i = x_i \in \mathbb{R}^d$, there exists a sequence of d -by- d orthogonal matrices $\{W_n\}_n$ such that*

$$n^{1/2} \left[(\mathfrak{M} - \tilde{P}) U_{\tilde{P}} S_{\tilde{P}}^{-1/2} \right]_h W_n \xrightarrow{\mathcal{L}} \mathcal{N}(0, \check{\Sigma}(x_i)),$$

where

$$\check{\Sigma}(x_i) := \frac{1}{m^2} \left(\sum_{\ell=1}^m \alpha^2(s, \ell) \right) \Delta^{-1} \mathbb{E} \left[(x_i^T X_j - (x_i^T X_j)^2) X_j X_j^T \right] \Delta^{-1} = \frac{1}{m^2} \left(\sum_{\ell=1}^m \alpha^2(s, \ell) \right) \Sigma(x_i)$$

is a covariance matrix that depends on x_i .

Proof. Following the proof of Lemma 6 in [26], for each $n = 1, 2, \dots$, choose orthogonal $W_n \in \mathbb{R}^{d \times d}$ so that $\mathbf{Z} = \mathbf{Z}^* W_n = U_{\tilde{P}} S_{\tilde{P}}^{1/2} W_n$. Dropping the explicit dependence on n , we rewrite the term $n^{1/2} \left[(M - \tilde{P}) U_{\tilde{P}} S_{\tilde{P}}^{-1/2} \right]_h W$ as follows

$$\begin{aligned} n^{1/2} \left[(\mathfrak{M} - \tilde{P}) U_{\tilde{P}} S_{\tilde{P}}^{-1/2} \right]_h W &= n^{1/2} \left[(\mathfrak{M} - \tilde{P}) U_{\tilde{P}} S_{\tilde{P}}^{-1/2} W \right]_h \\ &= n^{1/2} \left[(\mathfrak{M} - \tilde{P}) U_{\tilde{P}} S_P^{1/2} W W^T S_{\tilde{P}}^{-1} W \right]_h \\ &= n^{1/2} \left[(\mathfrak{M} - \tilde{P}) \mathbf{Z} \right]_h W^T S_{\tilde{P}}^{-1} W \\ &= \frac{n^{-1/2}}{m} \left[\mathfrak{M} \mathbf{Z} - \tilde{P} \mathbf{Z} \right]_h [n W^T S_P^{-1} W] \end{aligned} \quad (32)$$

The h -th scaled row of the matrix difference $\mathfrak{M} \mathbf{Z} - \tilde{P} \mathbf{Z}$ can be further expanded as

$$\begin{aligned} \frac{n^{-1/2}}{m} [\mathfrak{M} \mathbf{Z} - \tilde{P} \mathbf{Z}]_h &= \frac{n^{-1/2}}{m} \sum_{k=1}^{mn} (\mathfrak{M} - \tilde{P})_{hk} (\mathbf{Z})_k \\ &= \frac{n^{-1/2}}{m} \sum_{\ell=1}^m \sum_{j=1}^n \left(\mathfrak{M}_{i,j}^{(s,\ell)} - P_{ij} \right) X_j \\ &= \frac{n^{-1/2}}{m} \sum_{j \neq i} \left(\sum_{\ell=1}^m \mathfrak{M}_{i,j}^{(s,\ell)} - m P_{ij} \right) X_j - n^{-1/2} P_{ii} X_i, \end{aligned}$$

Conditioning on $X_i = x_i \in \mathbb{R}^d$, we first observe that

$$\frac{P_{ii}}{n^{1/2}} X_i = \frac{x_i^T x_i}{n^{1/2}} x_i \xrightarrow{a.s.} 0.$$

Moreover, the remaining portion of the scaled sum becomes

$$\begin{aligned}
& n^{-1/2} \sum_{j \neq i} \frac{1}{m} \left(\sum_{\ell=1}^m \mathfrak{M}_{i,j}^{(s,\ell)} - m(x_i^T X_j) \right) X_j \\
&= n^{-1/2} \sum_{j \neq i} \frac{1}{m} \left(\sum_{\ell=1}^m \left(\sum_{k=1}^m c_k^{(s,\ell)} A_{i,j}^{(k)} \right) - m(x_i^T X_j) \right) X_j \\
&= n^{-1/2} \sum_{j \neq i} \frac{1}{m} \left(\sum_{k=1}^m \underbrace{\left(\sum_{\ell=1}^m c_k^{(s,\ell)} \right)}_{:=\alpha(s,k)} A_{i,j}^{(k)} - m(x_i^T X_j) \right) X_j,
\end{aligned}$$

where $\sum_{k=1}^m \alpha(s, k) = m$ for all $s \in [m]$.

The above expression is a sum of $n-1$ independent 0-mean random variables, each with covariance matrix denoted by $\check{\Sigma}(x_i)$, computed as follows (suppressing the conditioning on $X_i = x_i$)

$$\begin{aligned}
\check{\Sigma}(x_i) &= \frac{1}{m^2} \mathbb{E} \left(\left(\sum_{\ell=1}^m \alpha(s, \ell) A_{i,j}^{(\ell)} - m(x_i^T X_j) \right)^2 X_j X_j^T \right) \\
&= \frac{1}{m^2} \mathbb{E} \left[\mathbb{E} \left[\left(\sum_{\ell=1}^m \alpha(s, \ell) A_{i,j}^{(\ell)} - m(x_i^T X_j) \right)^2 X_j X_j^T \mid X_j \right] \right] \\
&= \frac{1}{m^2} \mathbb{E} \left[\left(\mathbb{E} \left[\left(\sum_{\ell=1}^m \alpha(s, \ell) A_{i,j}^{(\ell)} \right)^2 \mid X_j \right] - m^2 (x_i^T X_j)^2 \right) X_j X_j^T \right] \\
&= \frac{1}{m^2} \mathbb{E} \left[\left(\left(\sum_{\ell=1}^m \alpha^2(s, \ell) \right) x_i^T X_j + \left(2 \sum_{k < \ell} \alpha(s, \ell) \alpha(s, k) - m^2 \right) (x_i^T X_j)^2 \right) X_j X_j^T \right] \\
&= \frac{1}{m^2} \left(\sum_{\ell=1}^m \alpha^2(s, \ell) \right) \mathbb{E} \left[(x_i^T X_j - (x_i^T X_j)^2) X_j X_j^T \right],
\end{aligned}$$

where the third equality holds because conditioning on $P = X X^T$,

$$\mathbb{E} \left[\sum_{\ell=1}^m \alpha(s, \ell) A^{(\ell)} \mid P \right] = m X X^T.$$

The fourth equality holds from the fact that conditioning on X_i and X_j ,

$$\mathbb{E}[(A_{i,j}^{(\ell)})^2 \mid X_i, X_j] = X_i^T X_j$$

for all $\ell \in [m]$ and

$$\mathbb{E}[A_{i,j}^{(k)} A_{i,j}^{(\ell)} \mid X_i, X_j] = \mathbb{E}[A_{i,j}^{(k)} \mid X_i, X_j] \mathbb{E}[A_{i,j}^{(\ell)} \mid X_i, X_j] = (X_i^T X_j)^2$$

for all $k \neq \ell$. Lastly, the fifth equality holds by simply observing that $\left(\sum_{\ell=1}^m \alpha(s, \ell) \right)^2 = m^2$.

By the multivariate central limit theorem we have that

$$n^{-1/2} \sum_{j \neq i} \frac{1}{m} \left(\sum_{\ell=1}^m \mathfrak{M}_{i,j}^{(s,\ell)} - m(x_i^T X_j) \right) X_j \xrightarrow{\mathcal{L}} \mathcal{N}(0, \check{\Sigma}(x_i)). \quad (33)$$

Next, recall (as in the proof of Theorem 1) $nW_n^T S_P^{-1} W_n \xrightarrow{a.s.} \Delta^{-1}$, so that by the multivariate version of Slutsky's theorem in Eq. (32) we get

$$n^{1/2} \left[(\mathfrak{M} - \tilde{P}) U_{\tilde{P}} S_{\tilde{P}}^{-1/2} \right]_h W_n \xrightarrow{\mathcal{L}} \mathcal{N}(0, \check{\Sigma}(x_i)),$$

where $\check{\Sigma}(x_i) = \Delta^{-1} \check{\Sigma}(x_i) \Delta^{-1}$.

Proof of Theorem 3. Fix the index $h \in [mn]$ as $h = n(s-1) + i$, where $s \in [m], i \in [n]$. Recall that for each $n = 1, 2, \dots$, we choose orthogonal $W_n \in \mathbb{R}^{d \times d}$ so that $\mathbf{Z} = \mathbf{Z}^* W_n = U_{\tilde{P}} S_{\tilde{P}}^{1/2} W_n$. With V_n defined as in Lemma 3, the matrix difference

$$n^{1/2} \left(U_{\mathfrak{M}_n} S_{\mathfrak{M}_n}^{1/2} - U_{\tilde{P}_n} S_{\tilde{P}_n}^{1/2} V_n \right)_h V_n^T W_n$$

can be decomposed into a sum of matrices (as shown in Eq.(31) of Theorem 5) as follows

$$n^{1/2} \left(U_{\mathfrak{M}_n} S_{\mathfrak{M}_n}^{1/2} - U_{\tilde{P}_n} S_{\tilde{P}_n}^{1/2} V_n \right)_h V_n^T W_n = n^{1/2} \left((\mathfrak{M}_n - \tilde{P}_n) U_{\tilde{P}_n} S_{\tilde{P}_n}^{-1/2} W_n \right)_h + n^{1/2} R_{h,n} W_n,$$

where $R_{h,n} \in \mathbb{R}^{mn \times d}$ is the residual matrix defined as $R = H_2 - H_3 + H_4 + H_5$. Further, in the proof of Theorem 5 it is shown that for any $i = 2, 3, 5$ we have

$$n^{1/2} \|H_i\|_{2 \rightarrow \infty} \leq \frac{Cm^{3/2} \log mn}{n^{1/2}} \quad \text{w.h.p.}$$

It remains to provide an appropriate bound for H_4 .

Rather than showing $\sqrt{n} \|H_4\|_{2 \rightarrow \infty}$ converges to 0 in probability, we will prove directly that $\sqrt{n} \|(H_4)_h\|_2$ converges to 0 in probability, which is sufficient. Adapting the exchangeability bound on the analogous term from [26], we recall that

$$\begin{aligned} H_4 &:= (I - U_{\tilde{P}} U_{\tilde{P}}^T) (\mathfrak{M} - \tilde{P}) Q^{(1)} S_{\mathfrak{M}}^{-1/2} \\ &= (I - U_{\tilde{P}} U_{\tilde{P}}^T) (\mathfrak{M} - \tilde{P}) (U_{\mathfrak{M}} - U_{\tilde{P}} U_{\tilde{P}}^T U_{\mathfrak{M}}) S_{\mathfrak{M}}^{-1/2} \\ &\quad + (I - U_{\tilde{P}} U_{\tilde{P}}^T) (\mathfrak{M} - \tilde{P}) (U_{\tilde{P}} U_{\tilde{P}}^T U_{\mathfrak{M}} - U_{\tilde{P}} V) S_{\mathfrak{M}}^{-1/2} \end{aligned}$$

Denote the first term in this expression via H_{41} (the second via H_{42}), and note that

$$\begin{aligned} H_{41} &:= (I - U_{\tilde{P}} U_{\tilde{P}}^T) (\mathfrak{M} - \tilde{P}) (U_{\mathfrak{M}} - U_{\tilde{P}} U_{\tilde{P}}^T U_{\mathfrak{M}}) S_{\mathfrak{M}}^{-1/2} \\ &= \underbrace{(I - U_{\tilde{P}} U_{\tilde{P}}^T) (\mathfrak{M} - \tilde{P}) (I - U_{\tilde{P}} U_{\tilde{P}}^T) U_{\mathfrak{M}} U_{\mathfrak{M}}^T (U_{\mathfrak{M}} S_{\mathfrak{M}}^{-1/2})}_{:= E_1} \\ H_{42} &:= (I - U_{\tilde{P}} U_{\tilde{P}}^T) (\mathfrak{M} - \tilde{P}) (U_{\tilde{P}} U_{\tilde{P}}^T U_{\mathfrak{M}} - U_{\tilde{P}} V) S_{\mathfrak{M}}^{-1/2} \\ &= (I - U_{\tilde{P}} U_{\tilde{P}}^T) (\mathfrak{M} - \tilde{P}) U_{\tilde{P}} (U_{\tilde{P}}^T U_{\mathfrak{M}} - U_{\tilde{P}} V) S_{\mathfrak{M}}^{-1/2} \end{aligned}$$

Considering first H_{41} , we have that

$$\|(H_{41})_h\|_2 \leq \|(E_1)_h\|_2 \|U_{\mathfrak{M}} S_{\mathfrak{M}}^{-1/2}\|.$$

Consider now the term $\|(E_1)_h\|_2$. As in [26], define the matrix operator (where for any symmetric matrix $B \in \mathbb{R}^{k \times k}$, we define $\Pi_d(B)$ to be the orthogonal projection onto the eigenspace corresponding to the eigenvectors of B with the d largest (in magnitude) eigenvalues). Similarly, let $\Pi_d^\perp(\mathbf{B})$ denote the orthogonal projection onto $(\Pi_d(B))^\perp$.

Note that for any permutation matrix Q , we have that

$$\begin{aligned} \Pi_d(QBQ^T) &= Q\Pi_d(B)Q^T \\ \Pi_d^\perp(QBQ^T) &= Q\Pi_d^\perp(B)Q^T. \end{aligned}$$

As in [26], for any $(B, H) \in \mathbb{R}^{k \times k} \times \mathbb{R}^{k \times k}$, define the operator $\mathcal{L}(B, H)$ via:

$$\mathcal{L}(B, H) = \Pi_d^\perp(H)(B - H)\Pi_d^\perp(H)\Pi_d(B)$$

Let us consider permutations $\tilde{Q} \in \mathbb{R}^{mn \times mn}$ of the form

$$\tilde{Q} = I_m \otimes Q$$

for permutations $Q \in \mathbb{R}^{n \times n}$. Note that, for such a \tilde{Q} , we have that

$$\tilde{Q}\mathfrak{M}\tilde{Q}^T = \begin{pmatrix} Q\mathfrak{M}^{(1,1)}Q^T & Q\mathfrak{M}^{(1,2)}Q^T & \dots & Q\mathfrak{M}^{(1,m)}Q^T \\ Q\mathfrak{M}^{(2,1)}Q^T & Q\mathfrak{M}^{(2,2)}Q^T & \dots & Q\mathfrak{M}^{(2,m)}Q^T \\ \vdots & \vdots & \ddots & \vdots \\ Q\mathfrak{M}^{(m,1)}Q^T & Q\mathfrak{M}^{(m,2)}Q^T & \dots & Q\mathfrak{M}^{(m,m)}Q^T \end{pmatrix},$$

and that for each (i, j) pair,

$$Q\mathfrak{M}^{(i,j)}Q^T = \sum_{\ell} c_{\ell}^{(i,j)} Q A^{(\ell)} Q^T.$$

Similarly,

$$\tilde{Q}\tilde{P}\tilde{Q}^T = J_m \otimes (QPQ^T).$$

Note that $\mathcal{L}(\mathfrak{M}, \tilde{P}) = E_1$, and as these orthogonal projections are unique, we have

$$\begin{aligned} \mathcal{L}(\tilde{Q}\mathfrak{M}\tilde{Q}^T, \tilde{Q}\tilde{P}\tilde{Q}^T) &= \tilde{Q}(I - U_{\tilde{P}}U_{\tilde{P}}^T)\tilde{Q}^T\tilde{Q}(\mathfrak{M} - \tilde{P})\tilde{Q}^T\tilde{Q}(I - U_{\tilde{P}}U_{\tilde{P}}^T)\tilde{Q}^T\tilde{Q}(U_{\mathfrak{M}}U_{\mathfrak{M}}^T)\tilde{Q}^T \\ &= \tilde{Q}E_1\tilde{Q}^T \end{aligned} \tag{34}$$

Since the rows of \mathbf{X} are i.i.d., together this implies that the matrix-pair entries of $(\mathfrak{M}, \tilde{P})$ are equal in distribution to those of $(\tilde{Q}\mathfrak{M}\tilde{Q}^T, \tilde{Q}\tilde{P}\tilde{Q}^T)$. Therefore, the entries of $\mathcal{L}(\tilde{Q}\mathfrak{M}\tilde{Q}^T, \tilde{Q}\tilde{P}\tilde{Q}^T) = \tilde{Q}E_1\tilde{Q}^T$ are equal in law to those of $\mathcal{L}(\mathfrak{M}, \tilde{P}) = E_1$. Therefore, for each row i we have that

$$\|(\tilde{Q}E_1)_i\|^2 = \|(\tilde{Q}E_1\tilde{Q}^T)_i\|^2 \stackrel{\mathcal{L}}{=} \|(E_1)_i\|^2,$$

which implies that for any $i, j \in [n]$ and $k \in [m]$,

$$\mathbb{E}(\|(\tilde{Q}E_1)_{(k-1)n+i}\|^2) = \mathbb{E}(\|(E_1)_{(k-1)n+j}\|^2) \quad (35)$$

Since this guarantees that

$$\mathbb{E}(\|(\tilde{Q}E_1)_{(k-1)n+i}\|^2)$$

depends only on k , and not on i , we can define for $i, j \in [n]$,

$$r_k := \mathbb{E}(\|(\tilde{Q}E_1)_{(k-1)n+i}\|^2) = \mathbb{E}(\|(E_1)_{(k-1)n+j}\|^2).$$

Observe that

$$\mathbb{E}(\|E_1\|_F^2) = \sum_{k=1}^m nr_k \geq n \max_k r_k.$$

Because $h = (s-1)n + i$, for $i \in [n]$, Eq.(35) and an application of Markov's inequality yield

$$\begin{aligned} \mathbb{P}(\sqrt{n}\|(E_1)_h\| > t) &\leq \frac{n\mathbb{E}(\|(E_1)_h\|^2)}{t^2} = \frac{nr_s}{t^2} \\ &\leq \frac{\mathbb{E}(\|E_1\|_F^2)}{t^2}. \end{aligned}$$

The entries of $\mathfrak{M} - \tilde{P}$ are bounded between $[-1, 1]$, and $(I - U_{\tilde{P}}U_{\tilde{P}}^T)U_{\mathfrak{M}}U_{\mathfrak{M}}^T$ is rank d (with spectral norm bounded by 1). Hence

$$\|E_1\|_F^2 \leq \|I - U_{\tilde{P}}U_{\tilde{P}}^T\|^2 \|\mathfrak{M} - \tilde{P}\|_F^2 \|(I - U_{\tilde{P}}U_{\tilde{P}}^T)U_{\mathfrak{M}}U_{\mathfrak{M}}^T\|_F^2 \leq m^2 n^2 d^2.$$

Now, we also have that, with high probability (so that the bad set has probability bounded above by Cn^{-2}), there exists a constant $C > 0$ such that

$$\begin{aligned} \|E_1\|_F^2 &\leq d^2 \|I - U_{\tilde{P}}U_{\tilde{P}}^T\|^2 \|\mathfrak{M} - \tilde{P}\|_2^2 \|(I - U_{\tilde{P}}U_{\tilde{P}}^T)U_{\mathfrak{M}}\|^2 \|U_{\mathfrak{M}}^T\|_F^2 \\ &\leq C \frac{m^4 n \log^2 mn}{n} = Cm^4 \log mn \quad \text{by Lemma 5, Eq.(A.3.1)} \end{aligned}$$

We then have that

$$\mathbb{E}(\|E_1\|_F^2) \leq C(m^4 \log mn + n^{-2}m^2 n^2 d^2) = C(m^4 \log mn + m^2 d^2).$$

Letting $t = n^{1/4}$ in our Markov bound, we see that $\mathbb{P}(\sqrt{n}\|(E_1)_h\| > n^{1/4}) \rightarrow 0$. As, w.h.p., we have that $\|U_{\mathfrak{M}}S_{\mathfrak{M}}^{-1/2}\| \leq C/\sqrt{mn}$, we have that

$$n^{1/2}\|(H_{41})_h\|_2 \leq n^{1/3}\|(E_1)_h\| n^{1/6}\|U_{\mathfrak{M}}S_{\mathfrak{M}}^{-1/2}\| \xrightarrow{P} 0.$$

Turning our attention to H_{42} , we have that (w.h.p.)

$$\begin{aligned} \|H_{42}\|_F &\leq \|(I - U_{\tilde{P}}U_{\tilde{P}}^T)(\mathfrak{M} - \tilde{P})(U_{\tilde{P}}U_{\tilde{P}}^T U_{\mathfrak{M}} - U_{\tilde{P}}V)S_{\mathfrak{M}}^{-1/2}\|_F \\ &\leq \|(I - U_{\tilde{P}}U_{\tilde{P}}^T)\| \cdot \|\mathfrak{M} - \tilde{P}\| \cdot \|U_{\tilde{P}}\| \cdot \|U_{\tilde{P}}^T U_{\mathfrak{M}} - V\|_F \|S_{\mathfrak{M}}^{-1/2}\| \\ &\leq C(m^{3/2}\sqrt{n \log mn}) \left(\frac{m \log mn}{n}\right) \left(\frac{1}{(mn)^{1/2}}\right) \leq C \frac{m^2 \log^{3/2} mn}{n}, \end{aligned}$$

where the last line follows from Lemmas 2, 5, and 3. Therefore, $n^{1/2}H_{42}$ converges to 0 in probability, and combined this yields that $n^{1/2}H_4$ converges to 0 as desired.

Since the matrix W_n is unitary, the bounds above imply that the term $n^{1/2}R_{h,n}W_n$ converges to 0 in probability. Moreover, by Lemma 6 we have

$$\lim_{n \rightarrow \infty} \mathbb{P} \left[n^{1/2} \left((\mathfrak{M} - \tilde{P}) U_{\tilde{P}} S_{\tilde{P}}^{-1/2} \right)_h W_n \leq x \right] \xrightarrow{\mathcal{D}} \int_{\text{supp} F} \Phi(x, \check{\Sigma}(y)) dF(y),$$

by integrating over the latent positions X_i . Finally, an application of Slutsky's theorem completes the proof.

B Proof of Theorem 4

We mimic the proof of Theorem 1 here, and so omit some detail. Conditioning on $X_i = x_i$, we write (where $\mathcal{R}_n = V_n^T W_n$ as defined in the proof of Theorem 3)

$$\begin{aligned} & n^{1/2} \left(\left(\hat{\mathbf{X}}_{\mathfrak{M}} V_n^T W_n \right)_{h_1} - \left(\hat{\mathbf{X}}_{\mathfrak{M}} V_n^T W_n \right)_{h_2} \right) \\ &= n^{1/2} \left(\left(\hat{\mathbf{X}}_{\mathfrak{M}} V_n^T W_n \right)_{h_1} - (\mathbf{Z}_n)_{h_1} + (\mathbf{Z}_n)_{h_2} - \left(\hat{\mathbf{X}}_{\mathfrak{M}} V_n^T W_n \right)_{h_2} \right) \\ &= n^{1/2} \left((\mathfrak{M}_n - \tilde{P}_n) \mathbf{Z} \right)_{h_1} + n^{1/2} R_{h_1,n} W_n - n^{1/2} \left((\mathfrak{M}_n - \tilde{P}_n) \mathbf{Z} \right)_{h_2} - n^{1/2} R_{h_2,n} W_n. \end{aligned}$$

Now,

$$\begin{aligned} & n^{1/2} \left((\mathfrak{M}_n - \tilde{P}_n) \mathbf{Z} \right)_{h_1} - n^{1/2} \left((\mathfrak{M}_n - \tilde{P}_n) \mathbf{Z} \right)_{h_2} \\ &= \frac{n^{-1/2}}{m} \left(\sum_{j \neq i} \left(\sum_{\ell=1}^m \mathfrak{M}_{i,j}^{(s_1, \ell)} - \mathfrak{M}_{i,j}^{(s_2, \ell)} \right) X_j \right) [n W_n^T S_P^{-1} W_n] \\ &= n^{-1/2} \left(\sum_{j \neq i} \frac{1}{m} \left(\sum_{\ell=1}^m \alpha(s_1, \ell) A_{i,j}^{(\ell)} - \alpha(s_2, \ell) A_{i,j}^{(\ell)} \right) X_j \right) [n W_n^T S_P^{-1} W_n]. \end{aligned}$$

Each of the $n-1$ terms, $\frac{1}{m} \left(\sum_{\ell=1}^m \alpha(s_1, \ell) A_{i,j}^{(\ell)} - \alpha(s_2, \ell) A_{i,j}^{(\ell)} \right) X_j$, is an independent, mean zero, random variable with covariance matrix given by (suppressing the conditioning on $X_i = x_i$)

$$\begin{aligned}
\Phi(x_i, s_1, s_2) &:= \frac{1}{m^2} \text{Cov} \left(\left(\sum_{\ell=1}^m \alpha(s_1, \ell) A_{i,j}^{(\ell)} - \sum_{\ell=1}^m \alpha(s_2, \ell) A_{i,j}^{(\ell)} \right) X_j \right) \\
&= \frac{1}{m^2} \mathbb{E} \left[\mathbb{E} \left[\left(\sum_{\ell=1}^m (\alpha(s_1, \ell) - \alpha(s_2, \ell)) A_{i,j}^{(\ell)} \right)^2 X_j X_j^T \middle| X_j \right] \right] \\
&= \frac{1}{m^2} \left(\mathbb{E}[\mathbb{E}[(x_i^T X_j) X_j X_j^T | X_j]] \sum_{\ell=1}^m (\alpha(s_1, \ell) - \alpha(s_2, \ell))^2 \right. \\
&\quad \left. + 2 \mathbb{E}[\mathbb{E}[(x_i^T X_j)^2 X_j X_j^T | X_j]] \sum_{k < \ell} (\alpha(s_1, k) - \alpha(s_2, k)) (\alpha(s_1, \ell) - \alpha(s_2, \ell)) \right) \\
&= \frac{1}{m^2} \sum_{\ell=1}^m (\alpha(s_1, \ell) - \alpha(s_2, \ell))^2 \mathbb{E}[(x_i^T X_j - (x_i^T X_j)^2) X_j X_j^T], \tag{36}
\end{aligned}$$

where the third equality holds because $\sum_{\ell=1}^m c_{\ell}^{(s,t)} = 1$ for any $s \in [m]$, and, as a consequence, $\left(\sum_{\ell=1}^m (\alpha(s_1, \ell) - \alpha(s_2, \ell)) \right)^2 = 0$, and hence

$$\sum_{\ell=1}^m (\alpha(s_1, \ell) - \alpha(s_2, \ell))^2 = -2 \sum_{k < \ell} (\alpha(s_1, k) - \alpha(s_2, k)) (\alpha(s_1, \ell) - \alpha(s_2, \ell)).$$

The multivariate CLT then provides that

$$n^{-1/2} \left(\sum_{j \neq i} \frac{1}{m} \left(\sum_{\ell=1}^m \alpha(s_1, \ell) A_{i,j}^{(\ell)} - \alpha(s_2, \ell) A_{i,j}^{(\ell)} \right) X_j \right) \xrightarrow{\mathcal{L}} \text{Norm}(0, \Phi(x_i, s_1, s_2)).$$

As $[nW_n^T S_P^{-1} W_n]$ converges a.s. to Δ^{-1} and each residual $(n^{1/2} R_{h_k, n} W_n$ for $k = 1, 2)$ converges in probability to 0, the result follows from multivariate Slutsky's and integrating over x_i . Finally, equating $\tilde{\Sigma}(x_i, \rho)$ from Theorem 1 with Eq. (36) yields the desired result.